Fisheries and Oceans Canada | Pêches et Océans Canada
Science | Sciences

Canadian Science Advisory Secretariat (CSAS)

Research Document 2014/090

Pacific Region

Comparison of the Fishery and Conservation Performance of Fixed- and Abundance-Based Exploitation Regimes for Coho Salmon in Southern British Columbia

Josh Korman[1] and Arlene Tompkins[2]

[1]Ecometric Research Inc. and Department of Zoology
University of British Columbia
3560 W 22nd Avenue
Vancouver, BC V6S 1J3

[2]Fisheries and Oceans Canada
3190 Hammond Bay Road
Nanaimo, BC V9T 6N7

November 2014

Canada

Foreword

This series documents the scientific basis for the evaluation of aquatic resources and ecosystems in Canada. As such, it addresses the issues of the day in the time frames required and the documents it contains are not intended as definitive statements on the subjects addressed but rather as progress reports on ongoing investigations.

Research documents are produced in the official language in which they are provided to the Secretariat.

Published by:

Fisheries and Oceans Canada
Canadian Science Advisory Secretariat
200 Kent Street
Ottawa ON K1A 0E6

http://www.dfo-mpo.gc.ca/csas-sccs/
csas-sccs@dfo-mpo.gc.ca

© Her Majesty the Queen in Right of Canada, 2014
ISSN 1919-5044

Correct citation for this publication:

Korman, J and Tompkins, A. 2014. Comparison of the Fishery and Conservation Performance of Fixed- and Abundance-Based Exploitation Regimes for Coho Salmon in Southern British Columbia. DFO Can. Sci. Advis. Sec. Res. Doc. 2014/090. viii +39p.

TABLE OF CONTENTS

ABSTRACT IV
RÉSUMÉ VI
1. INTRODUCTION 1
2. METHODS 2
2.1. Model Structure 2
2.1.1. Population Dynamics 2
2.1.2. Management Dynamics 4
2.2. Performance Measures 6
2.3. Model Parameterization 6
3. RESULTS 10
4. DISCUSSION 12
5. FISHERY MANAGEMENT SUMMARY 15
6. ACKNOWLEDGEMENTS 15
7. REFERENCES 1
8. TABLES 1
9. FIGURES 5

ABSTRACT

We compared a range of fixed- and abundance-based harvest policies for Coho salmon in Southern British Columbia using a simulation model. The model consisted of a two-stage (spawner-smolt, smolt-adult recruit) population dynamics component and a management component that simulated error in recruitment forecasts and harvest implementation, and was parameterized based on a meta-analysis of spawner-to-smolt stock recruitment data and information on marine survival rates from index stocks. The model simulated the dynamics of multiple populations of differing productivity and capacity within a management unit (MU). Performance under different harvest policies was evaluated based on simulated yield, inter-annual variability in yield, as well as metrics indexing the conservation status of individual populations. We simulated fixed harvest rates ranging from 0.1 to 0.8, abundance-based policies with a range of adult recruitment floors and ceilings, and harvest rates, and an abundance-based quota policy.

The maximum sustainable yield for the aggregate of populations within a management unit, assuming an average marine survival rate of 0.04, occurred at harvest rates ranging from 0.3-0.4. The inter-annual coefficient of variation (CV) in yield was relatively stable up to harvest rates of 0.3-0.4, after which it increased substantively due to overexploitation. Conservation failure rates increased rapidly with harvest rate with median values of 40% and 60% at harvest rates of 0.3 and 0.4, respectively. Extirpation rates were 5-fold higher at a harvest rate of 0.4 (ca. 50%) compared to 0.3 (ca. 10%).

Abundance-based harvest rates generally performed the same or slightly better than fixed harvest rate policies. More aggressive abundance-based policies (lower recruitment floors or ceilings) resulted in higher average harvest rates and poorer conservation performance compared to less aggressive policies. The weakness of abundance-based policies in general was their higher CV in catch. The PSC-type abundance-based harvest rate policy (three different harvest rates for three levels of status) generally performed as well as the continuous abundance-based policy that had the best conservation performance, but had slightly higher inter-annual variation in catch. The quota-based harvest policy had very poor performance. In most scenarios, the differences in yield and conservation measures between a fixed exploitation rate of 0.3 and the abundance-based harvest rate strategies with the best performance were not large.

Model performance was very sensitive to marine survival rate. Under the low survival regime (average survival of 0.01) none of the populations within the simulated management unit could be sustained, regardless of the harvest policy. This occurred because spawner-to-spawner productivity (α*MS*(1-H)) was on average less than one over the duration of each simulation, even for productive stocks. Not surprisingly, escapement and catch were much higher, and conservation and extirpation failure rates much lower, under the high marine survival regime (average=0.06). The difference in the conservation failure rates at a fixed exploitation rate of 0.3 or lower and any of the abundance-based policies was much greater under the high marine survival regime. This occurred because realized exploitation rates under abundance-based policies at high marine survival tended to be approximately 50%, resulting in a large relative increase in conservation failure rates for less productive stocks. Under abundance-based harvest policies, populations with lower productivity received less benefit from higher marine survival compared to more productive populations because harvest rates were higher.

Model performance was very sensitive to assumptions about conservation-related dynamics (Fig. 5). The conservation failure rate increased with the absolute level of the conservation limit, and increasing the limit at which extirpation occurred increased the extirpation rate and decreased escapement and catch. These results are not surprising and highlight the sensitivity

of the model to parameters that determine conservation dynamics that are highly uncertain. However, conservation and extirpation limits in general did not affect the relative performance across harvest policies.

Performance measures were generally insensitive to most assumptions about meta-population dynamics with the exception of straying. There was little effect of random vs. fixed stream length assignment to populations within an MU. The number of populations that were simulated did not influence the median response across trials, but increases did reduce the extent of inter-trial variation in response. Conservation performance improved as the extent of straying of returning spawners to non-natal populations increased. This occurred because strays from productive populations to less productive ones increased the overall escapement to the less productive populations. The extent of straying had little effect on the relative performance of alternate harvest policies within scenarios.

Performance measures were sensitive to the extent of inter-annual variation in marine survival rates, but relatively insensitive to the extent of temporal correlation or inter-population correlation in marine survival. The simulation analysis demonstrated that reductions in harvest implementation error through better in-season management can potentially lead to improvements in both conservation status of less productive populations and fisheries yields.

Performance measures were not sensitive to forecast error. This was expected for the fixed exploitation rate policies that do not depend on recruitment forecasts, but was surprising for abundance-based regimes that do. This insensitivity was caused by the fundamental flaw of using aggregate abundance to determine a harvest rate that protects less productive populations within the aggregate. An abundance-based rule that depends on the aggregate recruitment will still overexploit weak populations regardless of the error in recruitment forecasts. Overexploitation of these populations leads to reduced performance in terms of both conservation and yield.

In conclusion, abundance-based harvest rate rules only make sense if their limit reference points are based on the status of the weak populations that they are designed to protect. This analysis indicated that a fixed exploitation rate of 0.3 resulted in similar yield and conservation performance relative to abundance-based policies. Considering the higher inter-annual variation in yield associated with abundance-based policies and additional management costs required for implementation (e.g., recruitment forecasting), a fixed exploitation strategy of 0.3 was the optimal harvest policy that was examined. Although this conclusion was robust to a number of model assumptions, it is preliminary and is not a management recommendation. There is considerable uncertainty about the extent of depensation in spawner-to-smolt stock-recruitment relationships, the exchangeability of stock-recruitment parameters among MUs, and potential biases in meeting target harvest rates.

Comparaison du rendement des pêches et des activités de conservation relatives aux régimes d'exploitation fixes et fondés sur l'abondance du saumon coho dans le sud de la Colombie-Britannique

RÉSUMÉ

Nous avons comparé un éventail de politiques de récolte à taux fixe ou fondées sur l'abondance pour le saumon coho dans le sud de la Colombie-Britannique en utilisant un modèle de simulation. Le modèle consistait en une composante sur la dynamique des populations en deux phases (géniteur-saumoneau, saumoneau-recrue adulte) et en une composante de gestion qui simulait les erreurs dans les prévisions de recrutement et dans la mise en œuvre des récoltes; ce modèle était paramétré en fonction d'une méta-analyse des données de recrutement au stock « du géniteur au saumoneau » et en fonction de renseignements sur les taux de survie en mer de stocks indexés. Le modèle simulait la dynamique de multiples populations de productivité et de capacité différentes au sein d'une même zone de gestion (ZG). Le rendement sous différentes politiques de récolte a été évalué en fonction des rendements simulés, de la variabilité interannuelle de ces rendements ainsi que de mesures indexant l'état de conservation des populations individuelles. Les auteurs ont simulé des taux de récolte fixes allant de 0,1 à 0,8, des politiques basées sur l'abondance avec toute une gamme de seuils et de plafonds de recrutement des adultes ainsi que de taux de récolte, et une politique de quotas fondés sur l'abondance.

Le rendement maximal soutenu pour les populations en comigration faisant partie d'une même ZG, en supposant un taux de survie en mer moyen de 0,04, s'est produite à des taux de récolte allant de 0,3 à 0,4. Le coefficient de variation (CV) interannuelle du rendement était relativement stable jusqu'à des taux de récolte de 0,3 à 0,4 après quoi il augmentait considérablement en raison de la surexploitation. Les taux d'échec de conservation ont augmenté rapidement, les valeurs médianes étant de 40 % et de 60 % à des taux de récolte de 0,3 et 0,4, respectivement. Les taux de disparition étaient 5 fois supérieurs à un taux de récolte de 0,4 (env. 50 %) qu'à un taux de 0,3 (env. 10 %).

Les taux de récolte basés sur l'abondance ont généralement connu le même rendement, ou un rendement légèrement supérieur, que les politiques à taux de récolte fixe. Les politiques fondées sur l'abondance plus agressives (faibles seuils ou plafonds de recrutement) ont entraîné des taux de récolte moyens plus élevés et des rendements plus faibles sur le plan de la conservation en comparaison avec les politiques moins agressives. En général, la faiblesse des politiques basées sur l'abondance était leur CV plus élevé en matière de prises. La politique à taux de prises basée sur l'abondance de type CSP (trois différents taux de récolte pour les trois niveaux de statut tels que définies par la Commission du saumon du Pacifique) a généralement donné un rendement aussi bon que celui de la politique de récolte continue basée sur l'abondance qui a eu le meilleur rendement en matière de conservation, mais il y avait une plus grande variation interannuelle des prises. La politique de récolte basée sur les quotas a eu un rendement très faible. Dans la plupart des scénarios, les différences en termes de rendement et de mesures de conservation entre les stratégies prévoyant un taux d'exploitation fixe de 0,3 et celles prévoyant un taux de récolte fondé sur l'abondance ayant le meilleur rendement n'étaient pas importantes.

Le rendement des modèles était très sensible au taux de survie en mer. Dans le contexte d'un faible régime de survie (survie moyenne de 0,01), aucune des populations faisant partie de la ZG simulée ne pouvait être soutenue, peu importe la politique de récolte. Cela s'explique par le fait que la productivité « géniteur à géniteur » (α*MS*(1-H)) était, en moyenne, inférieure à 1 pour la durée de chaque simulation, même pour ce qui est des stocks productifs. Sans surprise,

les taux d'échappement et de prises étaient beaucoup plus élevés, et les taux d'échec de conservation et de disparition beaucoup moins élevés, sous le régime à taux de survie en mer élevé (moyenne = 0,06). Á un taux d'exploitation fixe de 0,3 ou moins et pour toutes les politiques basées sur l'abondance, la différence dans les taux d'échec de conservation était beaucoup plus grande dans le contexte d'un taux de survie en mer élevé. Cela s'explique par le fait que les taux d'exploitation concrétisés, dans le cadre des politiques fondées sur l'abondance à un taux de survie en mer élevé, avaient tendance à se chiffrer à 50 %, ce qui causait une importante augmentation relative des taux d'échec de conservation pour les stocks moins productifs. Dans le cadre des politiques de récolte fondées sur l'abondance, les populations à faible productivité bénéficiaient moins des taux de survie en mer élevés que les populations plus productifs puisque les taux de récolte étaient plus élevés.

Le rendement des modèles était très sensible aux hypothèses relatives aux dynamiques liées à la conservation (figure 5). Le taux d'échec de conservation a augmenté en même temps que le niveau absolu de la limite de conservation, et le fait d'augmenter la limite à laquelle les disparitions se réalisent n'a fait qu'augmenter le taux de disparition et diminuer les échappées et les prises. Ces résultats ne sont pas surprenants et soulignent la sensibilité du modèle aux paramètres très incertains qui déterminent la dynamique de la conservation. Cependant, en général, les limites de conservation et de disparition n'ont eu aucune répercussion sur le rendement relatif des politiques de récolte.

Les mesures du rendement étaient généralement insensibles à la plupart des hypothèses concernant la dynamique des métapopulations, à l'exception de l'errance. L'assignation d'une longueur de cours d'eau aléatoire ou fixe avait peu d'effet sur les populations d'une même ZG. Le nombre de populations simulées n'a pas influencé la réponse médiane pour l'ensemble des essais, mais les augmentations ont réduit l'ampleur des variations des réponses entre les essais. Le rendement de la conservation s'est amélioré à mesure que l'ampleur de l'errance des géniteurs en montaison vers les populations non natales a augmenté. Cela s'explique par le fait que les poissons errants provenant de populations productives et se retrouvant avec des populations moins productives augmentent en général les échappées vers les populations moins productives. L'ampleur de l'errance avait peu d'effet sur le rendement relatif des politiques de récolte proposées comme solutions de rechange aux scénarios.

Les mesures du rendement étaient sensibles à l'ampleur de la variation interannuelle des taux de survie en mer, mais relativement insensibles à l'ampleur de la corrélation temporelle ou de la corrélation entre les populations relativement à la survie en mer. L'analyse de la simulation a démontré que la réduction des erreurs dans la mise en œuvre des régimes de récolte grâce à une meilleure gestion en cours de saison pourrait mener à des améliorations de l'état de conservation des populations moins productives ainsi que de la production des pêches.

Les mesures du rendement n'étaient pas sensibles aux erreurs de prédiction. Ceci était prévu dans le cas des politiques à taux d'exploitation fixe qui ne dépendent pas des prévisions de recrutement, mais il s'agit d'une surprise dans le cas des régimes basés sur l'abondance qui, eux, en dépendent. Cette insensibilité a été causée par l'utilisation d'une abondance totale des populations en comigration afin de déterminer un taux d'exploitation qui protège les populations moins productives au sein de l'ensemble des populations en comigration, une faille fondamentale. Une règle fondée sur l'abondance qui dépend du recrutement de l'ensemble des populations en comigration entraînera tout de même une surexploitation des populations faibles, peu importe les erreurs dans les prévisions de recrutement. La surexploitation de ces populations entraîne un rendement réduit sur le plan de la conservation et de la production.

En conclusion, les règles de pêche avec taux de récolte fondés sur l'abondance ne sont utiles que si leurs points de référence limites sont basés sur l'état des populations faibles qu'elles

doivent protéger. Cette analyse a indiqué qu'un taux d'exploitation fixé à 0,3 donnait lieu à un rendement et un rendement de conservation similaires par rapport aux politiques fondées sur l'abondance. Considérant la plus grande variation interannuelle du rendement associée aux politiques fondées sur l'abondance et les coûts de gestion supplémentaires nécessaires à la mise en œuvre (p. ex., prévision du recrutement), une stratégie d'exploitation fixe de 0,3 est la politique de récolte optimale examiné dans cette étude. Même si cette conclusion était corroborée sous plusieurs des hypothèses du modèle, il s'agit d'un résultat préliminaire et non d'une recommandation en matière de gestion. Une grande incertitude persiste sur l'ampleur de l'effet dépensatoire des relations géniteur-saumoneau et stock-recrutement, l'interchangeabilité des paramètres stock-recrutement parmi les ZG, et à des biais possibles relatifs à l'atteinte de taux de récolte cibles.

1. INTRODUCTION

A group of populations with different productivities will exhibit highly divergent responses to a common harvest regime (Ricker 1958). For example, at an intermediate harvest rate, weak or unproductive populations will be depleted and possibly extirpated, while highly productive ones will be under-exploited. In many cases, such as for Coho salmon in southern British Columbia Bradford et al.. 2000, populations with varying productivity have considerable overlap in their temporal and spatial patterns of migration, and are therefore exposed to a common harvest regime. This represents a challenge for managers attempting to balance the trade-off between yield from the fishery and the conservation status of less productive populations. In this paper, we present a model that simulates this dynamic for Coho salmon in southern British Columbia. The main objective of the model is to quantify the yield-conservation trade-off and examine how it varies under alternate fixed- and abundance-based harvest rate policies and under various assumptions about population dynamics and management error.

Walters and Parma's (1996) simulation analysis concluded that abundance-based harvest policies provided only marginally better yields compared to fixed harvest rate strategies, and produced much higher inter-annual variation in yield. They also showed that the performance of abundance-based strategies degrade much more rapidly compared to fixed harvest rate policies as the extent of management error increases. When they considered the higher costs and challenges associated with accurately forecasting recruitment, they concluded that a fixed harvest rate policy is a better approach. This recommendation contrasts with the abundance-based policy that will be used to manage coho salmon in Southern BC if the fishery is reopened (Pacific Salmon Commission 2004). The rationale for the PSC policy is to allow some fishing but also promote rebuilding of coho stocks of conservation concern. Walters and Parma (1996) analysis was based on the recruitment dynamics of a single aggregate population and did not consider the status of weak population that are part of the aggregate when assessing policies. In this analysis, we develop a model that simulates the dynamics of multiple populations within a DFO management unit (MU) with a range of productivities to compare fishery and conservation performance under different harvest policies.

The model consists of a population dynamics component that uses a Beverton-Holt spawner-to-smolt stock-recruitment relationship that varies among populations within the MU. The number of returning pre-fishery recruits is predicted as the product of smolt production and marine survival rate for each population, aggregated across all populations in the MU. Random variation in freshwater and marine survival rates is simulated, and includes the effects of temporal autocorrelation and across-population correlations in deviations. A management component simulates an annual recruitment forecast for the MU that is used to determine exploitation rates for abundance-based harvest regimes, and also simulates implementation errors associated with realizing the target harvest rate. The number of spawners returning to each population's natal stream depends on the adult recruitment, realized harvest rates, and straying of spawners among populations within the MU. The model is used to evaluate harvest policies for populations in the Georgia Basin West management unit and the Thompson River drainage.

2. METHODS

2.1. MODEL STRUCTURE

2.1.1. Population Dynamics

The population dynamic component of the model simulates the abundance of coho in both freshwater and marine portions of their life cycle. We assumed juveniles migrate to the ocean as age-1+ smolts only and spend 1.5 years in the ocean before returning to spawning areas to complete a 3-yr life cycle. The model incorporates meta-population dynamics by simulating multiple populations through time within a set of theoretical streams, with exchange of individuals among populations determined by straying of returning spawners to streams other than the one they originated from. Adult recruitment is predicted based on the product of density-dependent smolt production and density-independent marine survival.

The number of smolts produced from a single population *i* in yr *t* of the simulation is predicted from a Beverton-Holt stock-recruitment curve for the freshwater component of the lifecycle,

(1) $$SM_{i,t} = \frac{(SP_{i,t-2})}{\frac{1}{\alpha_i} + \frac{SP_{i,t-2}}{\beta_i}} * e^{v_{i,t} - \frac{\sigma_f^2}{2}}$$

where, *SM* is the number of smolts produced from population *i*, *SP* is the number of returning spawners, α is the initial slope of the spawner-to-smolt stock-recruitment curve and is equivalent to the number of smolts produced per spawner at low density (stock productivity), β is the maximum number of smolts that can be produced from the population when stock size is not limiting (carrying capacity), and *v* is a random deviate drawn from normal distribution with a mean of 0 and standard deviations σ_f. Note that $\sigma^2/2$ term is a lognormal bias correction so that the mean of random deviates is approximately 0.

The adult recruitment potentially available to the fishery from each population one year later is predicted from,

(2) $$R_{i,t+1} = SM_{i,t} * MS * e^{\upsilon_{i,t} - \frac{\sigma_m^2}{2}}$$

where, *R* is the number of pre-fishery recruits from that population, *MS* is the average marine survival rate common to all populations, and υ is a random deviate in marine survival drawn from normal distribution with a mean of 0 and standard deviations σ_m.

On each simulation trial, freshwater stock-recruitment parameters for each population are randomly drawn from regional distributions estimated from a hierarchical meta-analysis (Korman and Tompkins 2014). To remove the effect of stream size on the carrying capacity estimates, data used in the meta-analysis were first standardized by the kilometers of accessible stream length for each stream. The carrying capacity term in eqn. 1 therefore represents the maximum smolts/km per population. Thus, prior to computation of eqn. 1, the predicted absolute number of spawners per population is converted to spawners/km, used to predict smolts/km via eqn. 1, and finally converted back to the total number of smolts produced from the population. These calculations are omitted from eqn. 1 for clarity of presentation. The total km of accessible habitat for the

management unit being simulated and the number of populations to simulate within the management unit were defined (see below) and held constant across all trials within a model scenario. The kilometers of accessible stream assigned to each population was however stochastically determined for each simulation trial, with the sum of stream lengths across populations always equivalent to the pre-defined total for the management unit. We assumed no relationship between the random assignment of freshwater productivities or length-standardized carrying capacity values for each population and the random assignment of stream lengths. We assume that within a simulation trial, the freshwater stock-recruitment relationship assigned to each population is stationary for the entire simulation period (e.g., 60 yrs). We also assume that the regional distribution of spawner-to-smolt stock-recruitment parameters developed from the meta-analysis of data from 16 streams in Korman and Tompkins (2014), represents the distribution of parameters for populations with the Georgia Basin West and part of the Interior Fraser (Thompson drainage) management units.

The total number of spawners returning to a population includes surviving individuals produced from that population as well as stray spawners that originated from other populations. To simulate this meta-population dynamic we first determine the number of spawners that will not return to their stream of origin ($ST_{i,t+1}$),

(3) $$ST_{i,t+1} = S_{i,t+1} * R_{i,t+1} * (1 - H_{i,t+1})$$

where S is the proportion of spawners that stray from each population (the straying rate) and H is the realized harvest rate on each population (see below). The straying rate is a function of spawner density in each stream calculated from,

(4) $$S_{i,t+1} = \frac{SP_{i,t+1}\delta}{SP_{i,t+1} + \phi}$$

where, δ is the maximum straying rate when spawner density in the natal stream is not limiting, and ϕ is the spawner density where the straying rate is 50% of the maximum. The total number of returning spawners to each population is calculated from,

(5) $$SP_{i,t+1} = R_{i,t+1} * (1 - H_{i,t+1}) * (1 - S_{i,t+1}) - \frac{km_i}{\sum_i km} \sum_i ST_{i,t+1}$$

where, km is the accessible stream length assigned to each population. The first 3 terms in eqn. 5 represents spawners that originated from population i, while the latter terms define the number of spawners straying to that population that originated from other populations. This number of strays to each population depends on the size of the stream assigned to that population relative to the total stream length for the management unit as well as the total number of strays produced from all populations. Populations that are randomly assigned to larger streams will receive a greater number of strays than those assigned to smaller streams. Note that our representation of populations is not spatially explicit, so straying does not depend on geographic proximity among simulated streams. While including such a dynamic would be more realistic, there is no data to spatially define both population structure and population dynamics parameters (i.e., α and β).

Depensatory mortality in freshwater survival rate is modeled using a threshold extinction limit,

(6)
$$SP_{i,t} = SP_{i,t} \mid SP_{i,t} \geq ExtLimit$$
$$SP_{i,t} = 0 \mid SP_{i,t} < ExtLimit,\ OR\ SP_{i,t} * km_i < 2$$

where, *ExtLimit* is the extirpation limit in units of spawners/km. Note that the number of spawners returning to a population in any year is set to zero in cases when the spawner density is lower than the extirpation limit or if the absolute number of spawners is less than two. We did not model depensation by using a depensatory spawner-to-smolt stock-recruitment relationship because there was no evidence for depensation in the meta-analysis of Korman and Tompkins (2014). However, the extirpation limit in eqn. 6 provides a crude means of accounting for depensation.

Random deviations in freshwater and marine survival rates are assumed to be lognormally distributed (Bradford 1995). Deviations are autocorrelated across years and across populations based on the following algorithm. First, temporally autocorrelated annual deviates common to all populations for freshwater and marines survival are computed from:

(7)
$$\nu_t = \nu_{t-1} * \rho_{y,f} + \mathrm{N}(0,\sigma_\nu) * \sqrt{(1-\rho_{y,f}{}^2)}$$

(8)
$$\upsilon_t = \upsilon_{t-1} * \rho_{y,m} + N(0,\sigma_\upsilon) * \sqrt{(1-\rho_{y,m}{}^2)}$$

where $\rho_{y,f}$ and $\rho_{y,m}$ are the lag-1 autocorrelation coefficients in deviates from the spawner-to-smolt relationship and deviates from the average marine survival rate, respectively. Note that when $\rho_y = 0$, there is no autocorrelation in survival rates. Population-specific deviates are then computed from the annual common deviates and the extent of correlation in deviates among populations from,

(9)
$$\nu_{i,t} = \nu_t * \rho_{p,f} + \mathrm{N}(0,\sigma_f) * \sqrt{(1-\rho_{p,f}{}^2)}$$

(10)
$$\upsilon_{i,t} = \upsilon_t * \rho_{s,m} + N(0,\sigma_m) * \sqrt{(1-\rho_{s,m}{}^2)}$$

where, $\rho_{p,f}$ and $\rho_{p,m}$ are the inter-population correlation coefficients based on the deviations from the spawner-to-smolt relationship and the average marine survival rate, respectively.

2.1.2. Management Dynamics

Harvest of adult recruits to the management unit is simulated using one of four methods: 1) a fixed harvest rate rule; 2) a continuous abundance-based harvest rate rule; 3) an abundance-based 'cut-off' harvest rate rule; or 4) an abundance-based 'cut-off' quota rule. The forecasted adult recruitment is used as the measure of management unit status to set harvest rate or quota in methods 2-3 and 4, respectively, and is simulated as the product of the actual simulated total recruits and deviates that depend on the magnitude of forecast error,

(11)
$$\hat{R} = R_t * e^{\kappa_t - \frac{\sigma_\kappa^2}{2}}$$

where, . R_t is the total pre-fishery recruitment to the management unit (the sum of the recruitments from each population) and κ_t is a random deviate from a normal distribution with a mean of 0 and a standard deviation σ_κ.

2.1.2.1. Fixed Harvest Rate Rule

Under this method, the target harvest rate each year (TH_t) is constant. For fixed harvest rate policies, we assumed the desired rate will be achieved through time-area closures and that recruitment forecasts are not needed to achieve the target rate. Thus, increasing the extent of recruitment error will not affect performance for scenarios based on fixed harvest rate policies.

2.1.2.2. Continuous Abundance-Based Harvest Rate Rule

Under this method, the target harvest rate each year is determined from:

$$
\begin{aligned}
TH_t &= H_{\min} \mid \hat{R}_t < R_{\min} \\
TH_t &= H_{\max} \mid \hat{R}_t > R_{\max} \\
TH_t &= H_{\min} + (\hat{R}_t - R_{\min}) \left[\frac{H_{\max} - H_{\min}}{R_{\max} - R_{\min}} \right] \mid E_{\min} \le \hat{R}_t \le R_{\max}
\end{aligned}
\tag{12}
$$

where, H_{min} and H_{max} are the minimum and maximum exploitation rates and R_{min} (recruitment forecast floor) and R_{max} (recruitment forecast ceiling) are the aggregate recruitment forecasts for the MU when those rates apply, respectively. As the target harvest rate depends on the recruitment forecast, this rule is potentially sensitive to the extent of forecast error. Harvest rates at intermediate escapements are determined by linear interpolation. Setting R_{min} =0 eliminates the recruitment floor, that is fishing continues regardless of how low the forecasted recruitment is.

2.1.2.3. Abundance-Based 'Cut-Off' (PSC) Harvest Rate Rule

The Pacific Salmon Commission (PSC 2004) has defined a harvest rate rule where the target harvest rate increases across three status categories (Low, Moderate, and Abundant). In the model, we assume that status is determined from the adult recruitment forecast. Note that abundance-based policy defined above (eqn. 12) is simply a continuous version of this three-level PSC policy. As for method 2, the PSC-harvest rate policy is sensitive to error in recruitment forecasts.

2.1.2.4. Abundance-Based 'Cut-off' Quota Rule

Under this method, the forecasted abundance of adult recruits is used to determine a catch quota (i.e., total allowable catch), rather than a harvest rate. Like the 'cut-off'-based PSC harvest rate rule, this method depends on three levels of status (forecasted adult recruitment). The realized target harvest is calculated as the ratio of the quota to the simulated number of actual recruits.

The average harvest rate applied across populations (H_t) is a product of the target harvest rate and a deviate that accounts for the error in attaining an average harvest rate,

$$
H_t = TH_t * e^{\lambda_t - \frac{\sigma_\lambda}{2}} \tag{13}
$$

where, λ_t is a random deviate from a normal distribution with a mean of 0 and a standard deviation σ_λ. This error reflects the difficulty in achieving the desired mean harvest rate on the aggregate population that would result from changes in the spatial and temporal distribution of the aggregate run as it passes through fishing areas and applies to all four harvest rate policies.

Population-specific harvest rates are calculated as the product of the mean harvest rate and a deviate that accounts for the variation in harvest rates among populations due to population-specific differences in run timing and holding patterns in relation to the time and area closures of the fishery,

(14) $$H_{i,t} = H_t * e^{\eta_t - \frac{\sigma\eta}{2}}$$

where, η_t is a random deviate from a normal distribution with a mean of 0 and a standard deviation σ_η. $H_{i,t}$ is substituted into eqn.'s 3 and 5 to determine in part the spawning escapement for each population. The total catch in each year for the management unit ($Total_Catch_t$) is simply the sum of catches across all populations,

(15) $$Total_Catch_t = \sum_{i=1} R_{i,t} * H_{i,t}$$

2.2. PERFORMANCE MEASURES

The performance of each harvest rate policy is evaluated based on five metrics that characterize the fishery in terms of average yield, interannual variation in yield, and the conservation status of the populations within the management unit. The metrics are:

1. the total catch from the MU, averaged across all years of the simulation
2. the coefficient of variation (CV) in total catch across years
3. the total escapement to the MU, averaged across years
4. the percentage of years where the population-specific spawning escapements are below a pre-determined conservation limit (spawners/km), averaged across all populations
5. the percentage of populations that are extirpated. A simulated population is extirpated whenever the number of spawners/km is less than the extirpation limit, or the absolute number of spawners is less than two, for three consecutive years.

The conservation failure metric aggregates performance across populations and is a compact measure of summarizing conservation status. Sustained periods of very low population size increase the risk of extirpation risk due to depensation and demographic stochasticity, and can also reduce genetic diversity that in turn can affect the ability of a population to persist. The conservation failure metric is intended to quantify this risk. In the simulation, there are no consequences associated with failing to meet the conservation limit. The extirpation limit represents the abundance below which a population cannot recover due to depensatory mortality. In the simulation, a cycle-line is terminated whenever its abundance drops below the extirpation limit or two spawners.

2.3. MODEL PARAMETERIZATION

Parameters for the population dynamics component of the simulation model were determined from an analysis of data from multiple populations or streams. The non-depensatory Beverton-Holt model was used as the default stock-recruitment function in the simulation because it had the best out-of-sample predictive power when applied to 16 streams in a hierarchical meta-analysis, and avoided biases in stock productivity and density dependent compensation apparent in other models (Korman and Tompkins

2014). On each simulation trial, stock productivity (α_i) and carrying capacity (β_i) parameters for each population are randomly selected from the marginal predictive posterior distributions of parameters developed from the hierarchical meta-analysis. As for α and β, we used the marginal predictive posterior distribution of the standard deviation around the stock-recruitment curve to simulate the extent of variation in freshwater survival rate (σ_f) for each population and trial. The lag-1 autocorrelation in annual deviates from the spawner-to-smolt relationships was estimated using the average lag-1 autocorrelation in the standardized Pearson residuals from the most likely stock-recruitment curves for each of the 16 populations ($\rho_{y,f}$ = 0.26, Table 1). The inter-population correlation was also estimated from the same standardized residuals ($\rho_{p,f}$ = 0.29, Table 1).

Data from DFO index streams from the South Coast and Thompson drainage were used to estimate a range of marine survival regimes to drive model simulations. We used estimates of marine survival rates from Georgia Basin West (GBW, Black, Big Qualicum) and Lower Fraser (LF, Salmon, Chilliwack, Inch) wild populations, and Thompson River hatchery populations (Lower, South, and North) for brood years (BY) 1987-2002 to develop the marine survival scenarios (see Table A2 of Korman and Tompkins 2014). First, data for GBW and Lower Fraser populations, or Thompson populations, were combined to develop two composite indices (GBW-LF, Thompson) following the methods described in Korman and Tompkins (2014). Only data from wild populations were used to compute the GBW-LF index. A wild composite index for the Thompson was created by multiplying the average annual Thompson hatchery survival rates by the annual ratio of wild-to-hatchery survival rates from GBW and LF data. The ratio was computed based on the annual average survival rate for Black and Salmon wild populations and the annual average survival rate of Big Qualicum, Chilliwack, and Inch hatchery populations. The average wild marine survival rates between brood years 1987 and 2002 for the GBW-LF and Thompson composite indices were 0.060 and 0.047, respectively. For the last 10 and 5 yrs of these records, average survival rates for GBW-LF and Thompson groups were 0.043 and 0.045 and 0.047 and 0.050, respectively. The average of the lowest 3 survival rates between 1987 and 2002 was 0.017 and 0.008 for GBW-LF and Thompson groups, respectively. Based on these estimates, we used average marine survival rates (MS of eqn. 2) of 0.01, 0.04, and 0.06 to represent poor, average, and good marine survival scenarios, respectively (Tables 1 and 2).

Parameters determining inter annual variation, serial autocorrelation, and inter-stock correlation in marine survival were computed based on data from BY 1987-2002. The standard deviations of log-transformed annual survival rates for the composite GBW-LF and Thompson stock groups were σ_m=0.57 and 0.93, respectively. The lag-1 autocorrelation in log-transformed survival rates for GBW-LF and Thompson groups over this period were $\rho_{y,m}$=0.57 and 0.20, respectively. The average inter-stock correlation between BY 1987 and 2002 for populations with a consistent time series over this period (Black, Salmon, Big Qualicum, Chilliwack, Inch, see Table A2 of Korman and Tompkins 2014) was $\rho_{p,m}$=0.71. It was not possible to compute $\rho_{p,m}$ based on Thompson data as only 3, generally non-overlapping time series of marine survival, were available (Lower, South, and North Thompson). Estimates of σ_m and $\rho_{y,m}$ for the Thompson aggregate are also considered unreliable for this reason. We therefore used values of σ_m and $\rho_{y,m}$ from the GBW-LF composite time series as default conditions for the Thompson drainage simulations (Tables 1 and 2).

There were not sufficient data to define separate sets of parameters for GBW and Thompson simulations. There were no spawner-to-smolt data from interior streams used in the analysis of Korman and Tompkins (2014). This analysis must therefore assume

that the marginal predictive distributions of freshwater stock-recruitment parameters apply to populations in both GBW and the Thompson drainage. The distributions appear to be relatively conservative for both areas, predicting a more rapid decline in spawner abundance under historic marine survival and harvest regimes than was evident in the SEDS escapement data (see Fig. 16 of Korman and Tompkins 2014). Marine survival trends from GBW and Thompson index streams were similar over the available time series and of similar scale in the last decade, and historical exploitation rates have also been very similar (see Fig. 15 of Korman and Tompkins 2014). Given the similarities in parameters for populations in GBW and the Thompson drainage, likely driven in part by data limitations, we used the same parameter estimates for both areas.

The total length of accessible rearing habitat in the GBW management unit and the Thompson drainage was estimated from the 1-50,000 digital Watershed Atlas (WA). Korman and Tompkins (2014) determined there are 1,335 and 2,268 km of accessible habitat in these areas, respectively. Based on a comparison of back calculated adult recruitment (from total escapement and estimates of exploitation rates for index stocks) and estimates derived from the product of accessible stream length, average smolt capacity per km of stream, and a range of historical marine survival rates, we concluded that the GBW habitat estimate was reasonable, but that the Thompson estimate produced too many smolts. By eliminating large mainstem reaches from the habitat calculation, accessible stream length for the Thompson was reduced to 1105 km. This value produced an adult recruitment that was reasonably close to historical estimates determined from escapements and was therefore used in this analysis. Considering the large uncertainty in the true amount of rearing habitat that limits Coho production in large areas such as the GBW MU or the Thompson drainage, we used an average value of 1200 km for both systems. This allowed us to reduce the number of scenarios to model.

The number of independent populations to simulate within the GBW management unit and the Thompson drainage was determined based on current hypotheses of population structure. For GBW, based on recommendations from a previous PSARC review, we assumed 24 independent populations, which on average would have an accessible stream length of 50 km each (Table 2). To further explore the effect of the number of populations on performance, we also simulated 50 populations each with an average accessible stream length of 24 km. For the Thompson, a minimum of three populations (Lower, South, and North) and a maximum of eight sub-populations have been proposed (see Table 3 of Interior Fraser Coho Recovery Team 2006). We modeled the latter case, resulting in an average accessible stream length per population of 150 km. The length of stream assigned to each population was randomly selected from a uniform distribution on each trial, with the constraint that the total of stream length across populations was 1200 km. Parameters determining straying of returning spawners among populations within a management unit are highly uncertain. We simulated a range of situations including no straying, low and high rates of straying that depended on returning spawner density, and density-independent straying (Table 2).

The absolute value of the conservation limit and the risk associated with not meeting the conservation limit at a particular frequency are both highly uncertain. We relied on previous studies focusing on reference points for Coho salmon to define the default conservation limit of 6 spawners/km used in this analysis (Tables 1 and 2). Stocker and Peacock (1998) proposed a conservation "floor" spawner density of 3 females/km for Canadian coastal Coho salmon populations. Chen et al. (2002) fit a depensatory Ricker stock-recruitment model to escapement and recruit data from the North Thompson River. They estimated that approximately 5,000 spawners are required to exceed the point where depensatory mortality occurs (S_{offset}). Standardizing this value by the number

of km of accessible habitat in the North Thompson (709 km, IFCRT 2006) leads to a limit of 6.6 spawners/km. Korman and Tompkins (2014) estimated that S_{offset} was 4.6 spawners/km based on a meta-analysis of spawner-to-smolt data from 16 streams. Note that this estimate was highly uncertain and substantially influenced by the prior distribution for S_{offset}, which was based on the estimate determined from Chen et al. (2002). We used a conservation limit of 6 spawners/km as a baseline conservation limit because it approximated the average of previously published estimates. The Recovery Potential Assessment for Interior Fraser Coho Salmon (DFO 2005) recommended that a minimum of 23,000 spawners are needed to ensure long-term survival of the Thompson River aggregate population. We therefore also explored the effects of using a higher conservation limit of 19 spawners/km (23,000 spawners/1,200 km of habitat) for one scenario (Table 2). The extirpation limit was arbitrarily set at 2 spawners/km, but we also explored a scenario with greater depensation in freshwater survival where the extirpation limit was 6 spawners/km.

We simulated fixed harvest rate policies ranging from 0.1 to 0.8 in increments of 0.1. There was very limited data to parameterize the management component of the model. Time series models are currently used to forecast marine survival for Coho populations in southern British Columbia. These models explain 50-60% of the variation in marine survival for Black Creek and the Salmon River (Simpson et al. 2004). A simulated value of σ_κ=0.5 is required to generate the same correlation given the assumed error structure (Table 1). However, the extent of this error should be considered conservative of the true uncertainty in recruitment forecasts because adult recruitment will also depend on aggregate smolt production, which is only measured at a few index streams within each management unit. Current recruitment forecasts do not consider escapement or smolt production data. Thus, we also simulated a higher level of recruitment forecast error of 1. We also simulated σ_κ=0 to evaluate performance under the ideal situation where there is no error in forecasting. There were no data available to estimate the extent of error in attaining the target harvest rate (implementation error) averaged over all populations, and the extent of variation in harvest rates applied to individual populations. We simulated arbitrary σ_λ and σ_η values of 0, 0.25, and 0.5 (Tables 1 and 2).

Abundance-based policies were simulated using a range of recruitment forecast floors and ceilings, and harvest rates. The recruitment forecast floor at which the minimum harvest rate is used (R_{min}) was set 7,200 or 25,000 fish (Table 2). The former limit is equivalent to the number of spawners required to meet the absolute conservation limit for the aggregate population (7,200 = 6 spawners/km * 1200 km of accessible stream length) for the Thompson drainage. The latter value is equivalent to the conservation reference point for the Thompson from Irvine et al. (2001, 25% of the historical peak spawner abundance) and is equivalent to a spawner density of approximately 20 fish/km. The recruitment forecast ceiling at which the maximum harvest rate is used (R_{max}) was arbitrarily set at 25% (25000), 50% (48000), and 75% (73000) of adult carrying capacity at equilibrium under default conditions (97000, see below). The harvest rate at the escapement floor (H_{min}) was set at 0.1 based on the assumption that some coho will be harvested incidentally as bycatch in sport and commercial fisheries even when the southern BC commercial coho fishery is closed. The harvest rate at the escapement ceiling (H_{max}) was set to 0.6. In total, six continuous abundance-based harvest policies were evaluated.

We simulated a three-level abundance-based harvest rate rule (i.e., PSC-type harvest rate) using low, moderate, and high abundance categories defined by 25%, 50%, and 75% of adult carrying capacity. Harvest rates of 0.1, 0.3, and 0.6 were applied within each of these abundance categories, respectively. These are the approximate midpoints

of the range of harvest rates provided in the 1999 Pacific Salmon Treaty (PSC 2008). A PSC-type quota rule was also simulated using quota values of 9700, 29000, and 58000, which were determined by multiplying PSC harvest rates of 0.1, 0.3, and 0.6 by the predicted equilibrium adult carrying capacity. In total, we simulated 16 alternate harvest rate policies (8 fixed rate, 6 continuous abundance-based, 1 PSC-type abundance-based, and 1 PSC-type quota based).

A total of 60 years was simulated for each trial. Each population was seeded with 20% of the number of spawners required to meet carrying capacity. Carrying capacity for both GBW and Thompson units was assumed to be 97,000 spawners, estimated as the product of the length of accessible habitat (1200 km), the maximum smolts produced per km when spawning stock size is not limiting (2022, from Korman and Tompkins 2014) and an assumed future marine survival rate of 0.04 (ca. historical average over last 10 years). The initial seeding rate of 20% starts the simulation with approximately 20,000 spawners, similar to average escapements to the Thompson drainage over the last decade (see Fig. 13, Korman and Tompkins 2014). The current total escapement to GBW over the last decade has likely been much larger than this, but consists of a large and unknown hatchery component that may make little contribution to smolt production. The effective Coho escapement to the GBW MU is therefore highly uncertain, so we assume the relative initial seeding rate for the simulation is equivalent to that used for the Thompson. Performance statistics were computed using the entire 60-yr time series, which is equivalent to 20 Coho salmon generations. 1000 trials were simulated for each harvest policy and box plots were used to summarize the distribution of performance measure values.

3. RESULTS

There was a strong positive correlation among conservation performance measures, and an inverse correlation between fishery and conservation performance (Fig. 1). Under a fixed exploitation strategy where target harvest rates ranged from 0.1-0.8, the aggregate escapement to the MU decreased as harvest rate increased and conservation failure rate and the proportion of populations that were extirpated increased. The median escapement across 1000 trials explained 97% and 90% of the variation in median conservation failure and extirpation rates, respectively, and the conservation failure rate explained 97% of the variation in the extirpation rate. The maximum sustainable yield for the aggregate, based on the median of 1000 trials of average catch (over 60 years of simulation per trial), was approximately 7500 fish and occurred at harvest rates ranging from 0.3-0.4. The inter-annual coefficient of variation (CV) in catch was relatively stable up to harvest rates of 0.3-0.4, after which it increased substantively due to overexploitation. Conservation failure rate increased rapidly with harvest rate with median values of 40% and 60% at harvest rates of 0.3 and 0.4, respectively. Median extirpation rates were 5-fold higher at a harvest rate of 0.4 compared to 0.3.

Abundance-based harvest rates generally performed the same or marginally better than fixed harvest rate policies. More aggressive abundance-based policies (e.g., R_{min}=7.2 k, R_{max}=25 k) resulted in higher average harvest rates and poorer conservation performance compared to less aggressive policies (e.g., R_{min}=25 k, R_{max}=73 k, Fig. 2). Across abundance-based policies, the one with the lowest recruitment floor and highest recruitment ceiling (R_{min}=7.2 k, R_{max}=73 k) produced the highest catch, had marginally better conservation performance, and very low extirpation rates. However, all abundance-based policies had higher CVs in catch compared to fixed harvest rate policies. The PSC-type abundance-based harvest rate policy (PSC-H) generally performed as well as the optimal continuous abundance-based policy (R_{min}=7.2 k,

R_{max}=73 k) but had higher inter-annual variation in catch. The quota-based harvest policy (PSC-Q) had very poor performance. This occurred because the quota at the lowest stock size category generally resulted in exploitation rates that were much too high for less productive populations. This drove future recruitments down, leading to even higher exploitation rates focused on the remaining productive stocks. Ultimately this dynamic led to extirpation of all simulated stocks in a given trial.

Model performance was very sensitive to marine survival rate. Under the low survival regime (Fig. 3) none of the populations within the simulated management unit could be sustained, regardless of the harvest policy. This occurred because the net spawner-to-spawner productivity (α*MS*(1-H)) was on average less than one over the duration of each simulation, even for very productive populations. Not surprisingly, escapement and catch were much higher, and conservation and extirpation failure rates much lower, under the high marine survival regime (Fig. 4). At higher marine survival, abundance-based harvest rate policies generally had yields similar to those based on fixed exploitation rates of 0.3 or 0.4. However, there was a much bigger improvement in the conservation failure rate under higher marine survival for fixed exploitation strategies than for abundance-based ones. For example, at a fixed rate of 0.3, the median conservation failure rate declined from 40% under average marine survival, to less than 10% under high marine survival. In contrast, for the optimal abundance-based policy (R_{min}=7.2 k, R_{max}=73 k), conservation failure declined from 40% at high marine survival to 20% under average survival. Differences in the relative improvement in conservation failure rate across survival regime-harvest policy occurred because realized exploitation rates for abundance-based policies at high marine survival tended to be approximately 50%, resulting in a larger relative increase in conservation failures for less productive stocks.

Increasing the conservation limit from 6 spawners/km to 19 spawners/km and the extirpation rate from 2 spawners/km to 6 spawners/km (Table 2) substantially increased conservation failure and extirpation rates (Fig. 5). Escapement and catch declined under the more sensitive conservation scenario because a greater fraction of populations were extirpated due to the higher extirpation limit. In general, differences among harvest rate policies were similar under the more sensitive conservation scenario relative to the default one, and all had very high conservation failure and extirpation rates. There was virtually no difference among scenarios where stream lengths were assigned randomly to populations with a simulation relative to the scenario where streams lengths were fixed and equal among populations (Fig. 6). Increasing the number of populations from 8 to 24 (Fig. 7) to 50 (Fig. 8) resulted in less inter-trial variation in performance, but no visible difference in relative performance among harvest policies.

Performance measures were moderately sensitive to the extent of straying of returning spawners to non-natal populations. In the absence of straying, extirpation rates were considerably higher and there was a marginal increase in conservation failure rates (Fig. 9). This occurred because strays from productive populations to less productive populations increase the escapement to the latter, so in the absence of straying, conservation performance declined. The opposite occurred when straying rate was increased (Fig. 10) or when straying was assumed to be density independent (Fig. 11). In the latter case, average straying rates over a simulation tended to be higher because they were independent of density, leading to slight improvements in conservation performance.

Performance measures were sensitive to the extent of inter-annual variation in marine survival rate, but relatively insensitive to temporal and inter-population correlation in marine survival. Escapement and catch declined, while conservation failure rate,

extirpation rate, and variation in catch increased under the scenario with higher variation in marine survival (Fig. 12). Conservation metrics were most sensitive to higher variation in marine survival, and both fixed and abundance-based harvest rate policies were affected. In contrast, there was little effect of higher temporal autocorrelation in marine survival rates (Fig. 13) or greater covariation in survival rate among populations (Fig. 14).

The response of the model to the extent of management error was variable over error types and harvest policies. As expected, performance for fixed harvest rate policies were identical when forecast error was eliminated (Fig. 15) or doubled (Fig. 16). This occurred because the model assumes that harvest rates are achieved through in-season methods rather than through pre-season recruitment forecasts, and hence do not depend on the forecast. Abundance-based harvest policies were also insensitive to the extent of forecast error. Eliminating harvest implementation error led to slightly increased catch and reduced conservation failure rates for most abundance-based harvest policies (Fig. 17). Doubling the extent of implementation error led to an opposite and stronger response (Fig. 18).

4. DISCUSSION

We compared the conservation and fishery performance of a range of fixed- and abundance-based harvest regimes using a simulation model. Although there is a considerable history of simulation-based harvest policy evaluation (see Hilborn and Walters 1992), our effort was relatively unique because it considered the variation in productivity among populations that experience a common harvest regime. The analysis suggests that a maximum sustainable yield for Coho salmon in southern BC is achieved at fixed harvest rates ranging from 0.3-0.4. This range also provided maximum yields under the higher marine survival regime. It was not possible to evaluate the optimal fixed harvest rate under the low marine survival regime because all populations were extirpated even under the lowest exploitation rate of 0.1. We explored a slightly improved low marine survival regime with an average rate of 0.02. Although not shown for brevity, optimal yields still occurred at fixed rates of 0.3-0.4. It is worth noting that this exploitation range is approximately half the rate that populations in southern BC were harvested at prior to the closure of the Coho salmon fishery (see Fig. 12 of Korman and Tompkins 2014). Lower harvest rates improved conservation performance (Fig. 1). Harvest rates greater than 0.3 resulted in a rapid increase in the fraction of stocks that were extirpated, and extirpation rates at harvest rates less than 0.3 were very low. Extirpation and conservation failure rates were much higher when marine survival was low (Fig. 3) or when there was stronger depensation in freshwater survival rate (Fig. 5).

Abundance-based harvest rate policies had similar or marginally better overall performance than fixed harvest rate policies in terms of both average catch and conservation statistics, but at the cost of higher inter-annual variation in catch (Fig. 2). In most scenarios, the differences in average catch and conservation measures between a fixed exploitation rate of 0.3 and the abundance-based policy with the best performance in terms of yield and conservation were not large. This occurred because most of the abundance-based rules we evaluated had median realized harvest rates that were very similar to 0.3.

The quota policy that we evaluated had very poor performance. In years of low returns, the quota for the lowest status category was still high enough to result in exploitation rates that were too high for some populations. This led to reductions in future recruitment leading in turn to even higher exploitation rates on the remaining more productive

populations. In the long term, this dynamic led to the extirpation of all populations within the management unit. Policies with much lower quotas would have had better conservation performance than the single policy we evaluated. For brevity, we did not evaluate additional quota policies, as difficulties with quota management in fisheries with high forecast error are already well recognized. This analysis has highlighted an additional problem with the long-term viability of quota management in the setting of mixed-stock fisheries.

Effects of marine survival on model performance generally followed expected responses, but there was an interesting exception. Not surprisingly, catch and escapement increased, and conservation failure and extirpation rates decreased, under the high marine survival regime (Fig. 4). However, there was a much bigger relative improvement in conservation performance under higher marine survival for fixed exploitation strategies than for abundance-based ones. For example, at a fixed exploitation rate of 0.3, the median conservation failure rate declined from 40% under average marine survival, to less than 10% under high marine survival. In contrast, for the optimal abundance-based policy (R_{min}=7.2 k, R_{max}=73 k), conservation failure declined from 40% at high marine survival to 20% under average survival. This two-fold difference in the relative improvement in conservation failure rate under higher marine survival across harvest policies occurred because the aggregate abundance was higher when marine survival was higher, resulting in application of the maximum harvest rate (R_{max}=0.6) in most years of the simulation. Thus, under abundance-based harvest regimes, populations with lower productivity received less benefit from higher marine survival compared to more productive populations because harvest rates are higher, which in turn reduces recovery rate of less productive populations.

Model performance was very sensitive to assumptions about conservation-related dynamics (Fig. 5). The conservation failure rate increased with the absolute level of the conservation limit, and increasing the limit at which extirpation occurred increased the extirpation rate and decreased escapement and catch. These results are not surprising and highlight the sensitivity of the model to parameters that determine conservation dynamics (e.g., depensatory mortality) that are highly uncertain. However, conservation and extirpation limits in general did not affect relative performance across harvest policies.

Performance measures were generally insensitive to most assumptions about meta-population dynamics with the exception of straying. There was no effect of random versus fixed assignment of stream lengths (across trials) to each population (Fig. 6). This occurred because we did not simulate systematic trends, such as assigning larger streams to more productive populations. This particular situation would increase the trade-off between catch and conservation metrics. As expected, increasing the number of populations that were simulated reduced inter-trial variance in performance measures, but not the central tendency of the distributions (Fig.'s 7 and 8). Conservation performance improved as the extent of straying of returning spawners to non-natal populations increased. (Fig.'s 9-11). This occurred because strays from more productive populations to less productive ones increased escapement to the less productive populations and therefore improved overall conservation performance within the MU. We are highly uncertain about parameters that determine the extent of straying. However, similar to the conclusion from the sensitivity analysis of conservation and extirpation limits, straying parameters had little effect on the relative performance of alternate harvest policies within scenarios.

Performance measures were sensitive to the extent of inter-annual variation in marine survival rate, but relatively insensitive to the extent of temporal correlation or inter-

population correlation. Escapement and catch declined, while conservation failure rate, extirpation rate, and variation in catch increased under the scenario with higher variation in marine survival (Fig. 12). This occurred because higher variation in survival rates increased the frequency of very low survival rates in some years that reduced escapement to the point where it limited future recruitment. This effect was not fully compensated by the increased frequency of higher survival rates because of density dependent limitation in smolt production at higher escapements. As for many other model parameters, relative performance among harvest policies was similar under the default and high marine survival rate variation scenarios.

The simulation analysis demonstrated that reductions in harvest implementation error through better in-season management can potentially lead to improvements in both conservation status of weak populations and fisheries yields (Fig. 17). The extent of improvement depends on the relative variance of management and process errors as well as other aspects of population dynamics. There is a limit to how much catch and conservation statistics can be improved by reducing implementation error given the assumed extent of natural variation and the fact that a common target harvest rate is being applied to populations with a range of productivities. When implementation error was high (Fig. 18), its effects began to dominate and performance was degraded. Unfortunately, because the simulated implementation errors used here were arbitrarily defined due to lack of data, it is uncertain where the simulated values lie relative to the management error associated with a future fishery. In some fisheries, realized harvest rates tend be higher than target rates, and the extent of this bias has been shown to increase when recruitment is lower (Holt and Peterman 2006). We did not attempt to simulate this dynamic as there are no data to estimate historical harvest implementation error rates, let alone a relationship between implementation error and recruitment.

Performance measures were not sensitive to forecast error (Fig.'s 15-16). This was expected for the fixed exploitation rate policies that did not depend on recruitment forecasts in the model, but was surprising for abundance-based regimes that did. This insensitivity was caused by the fundamental flaw of using aggregate abundance to determine harvest rate to protect less productive populations within the aggregate. An abundance-based rule that depends on the aggregate recruitment will still overexploit weak populations regardless of the error in recruitment forecasts. Higher forecast error does not change the long-term average target exploitation rate, and hence has little effect on conservation performance.

This analysis indicated that a fixed exploitation rate of 0.3 resulted in similar yield and conservation performance compared to the optimal abundance-based regimes that were considered. Abundance-based policies resulted in much higher inter-annual variation in yield and would be more expensive to implement than fixed harvest rate regimes. Thus, of all the harvest policies we examined, a fixed exploitation rate of 0.3 had the best overall performance. This conclusion should be considered preliminary and is not a management recommendation. There is considerable uncertainty about the potential for depensation in spawner-to-smolt stock-recruitment relationships, the exchangeability of stock-recruitment parameters among MUs, and potential biases in achieving target harvest rates. In addition, recommendations on harvest policies need to be made by policy-makers that are tasked with balancing the trade-offs between fisheries performance and conservation.

Our model simulated populations of varying productivity within a management unit only. The current closure of the southern BC Coho salmon fishery is largely based on the status of the interior Fraser MU, even though the fishery was and would be supported by populations from multiple MUs in southern BC. In addition, the status of Coho salmon in

the IF MU affects fisheries in Puget Sound and even fisheries on other salmon species. The utility of the analysis presented here for management could therefore be improved by substituting MU-specific fishery performance measures (catch and CV of catch) with those from larger areas or other species that are affected by the status of the MU that is modelled. The modeling framework currently does not account for such larger-scale considerations, but is still a useful tool to evaluate the effects of harvest policies on the conservation status within an MU.

5. FISHERY MANAGEMENT SUMMARY

Fisheries management requires a model to evaluate harvest regimes that are responsive to resource status in order to implement the PST Southern Coho Management Plan (Annex IV Chapter 5, PSC 2004). The specific requirements of such a model and its application in relation to the model and analysis developed here are described below.

1. ***Method for biologically determining the categorical status of the Key MU's.*** The model uses simulated adult recruitment forecasts to define simulated harvest rates. We compared fishery and conservation performance under a range of harvest regimes and scenarios describing population dynamics and management error. Results demonstrate trade-offs between fishery and conservation performance, which will be helpful to define the benefits of categorical status-based harvest regimes.
2. ***Sufficient flexibility in technical capabilities and available information to overcome data limitations (stock abundance and escapement) in implementing the plan.*** By assuming exchangeability in model parameters among MUs that define population dynamics, and by using a GIS database to estimate smolt carrying capacity that is available for the entire province, the model can theoretically be applied to any management unit within BC. However, the assumption of exchangeability is uncertain, and results should be used with caution.
3. ***An objective basis for monitoring, evaluation, and modifying the management regimes.*** This modeling effort provides no information for monitoring harvest management regimes, but does provide an objective basis for examining their potential performance.
4. ***Application to southern BC MUs (GBW and IF) to determine MU-specific reference points related to abundance levels (or other measures of status).*** The model was used to evaluate a range of abundance-based reference points that determine harvest rates as well as fixed exploitation rate strategies. A range of scenarios were simulated that include current hypothesis of meta-population structure for both GBW and IF (Thompson drainage only) MUs.

6. ACKNOWLEDGEMENTS

Thanks to Blair Holtby, Mike Bradford, Michael Folkes, Jim Irvine, Michael Chamberlain, Kent Simpson, Eric Parkinson, Joseph Tadey, Gary Morishima, and Bob Hayman for providing data or useful commentary on this analysis.

7. REFERENCES

Bradford, M.J., Myers, R.A., and J.R. Irvine. 2000. Reference points for coho salmon *(Oncorhynchus kisutch)* harvest rates and escapement goals based on freshwater production. Can. J. Fish. Aquat. Sci. 57: 677-686.

Bradford, M.J. 1995.Comparative review of Pacific salmon survival rates.. Can. J. Fish. Aquat. Sci. 52: 1327-1338.

Chen, D.G., and L.B. Holtby. 2002. A regional meta-model for stock-recruitment analysis using an empirical Bayesian approach. Can. J. Fish. Aquat. Sci.. 59: 1503-1514.

Hilborn, R. and C.J. Walters. 1992. Quantitative fisheries stock assessment. Chapman and Hall, New York, NY.

Holt, C.A., and R.M. Peterman. 2006. Missing the target: uncertainties in achieving management goals in fisheries on Fraser River, British Columbia, sockeye salmon *(Oncorhynchus nerka)*. Can. J. Fish. Aquat. Sci. 63: 2722-2733.

Interior Fraser Coho Recovery Team. 2006. Conservation strategy for Coho salmon *(Oncorhynchus kisutch)*, interior Fraser River populations. Fisheries and Oceans Canada.

Irvine, J.R., C.K. Parken, D.G. Chen, J. Candy, T. Ming, J. Supernault, W. Shaw, and R.E. Bailey. 2001. Stock Assessment of Coho Salmon from the Interior Fraser River. DFO Can. Sci. Advis. Sec. Res. Doc. 2001/083. 67 p.

Korman, J. & A. Tompkins. 2014. Estimating Regional Distributions of Freshwater Stock Productivity, Carrying Capacity, and Sustainable Harvest Rates for Coho Salmon Using a Hierarchical Bayesian Modelling. DFO Can. Sci. Advis. Sec. Res. Doc. 2014/089. vii + 54 p

PSC (Pacific Salmon Commission). 2008. Pacific Salmon Treaty, March 2004. 116 pp.

Simpson, K., Chamberlain, M., Fagan, J., Tanasichuk, R.W., and D. Dobson. 2004. Forecast for southern and central British Columbia coho salmon in 2004. DFO Can. Sci. Advis. Sec. Res. Doc. 2004/135. viii + 69 p.

DFO. 2005. Recovery Potential Assessment for Interior Fraser Coho Salmon *(Oncorhynchus kisutch)*. DFO Can. Sci. Advis. Sec. Sci. Advis. Rep. 2005/061.

Ricker, W.E. 1958. Maximum sustained yields from fluctuating environments and mixed stocks. J. Fish. Res. Bd. Can. 15:991-1006.

Stocker, M. and D. Peacock. 1988. Report of the PSARC Salmon Subcommittee meeting April 27-May 1, 1998. and the Steering Committee meeting May 4, 1998. Canadian Stock Assessment Proceedings Series 98/08. Fisheries and Oceans Canada, Ottawa, Onto.

Walters, C.J., and A.M. Parma. 1996. Fixed exploitation rate strategies for coping with effects of climate change. Can. J. Fish. Aquat. Sci. 53:148-158.

8. TABLES

Table 1. Summary of default model parameters. SD denotes standard deviation. The 'i' subscript for spawner-to-smolt stock-recruitment parameters α and β denote that values are stochastic draws for each population within a trial. Values in parentheses represent non-default values that were evaluated in sensitivity analyses.

Symbol	PARAMETER	VALUE	Source
	POPULATION DYNAMICS PARAMETERS		
α_i, β_i	Spawner-to-smolt productivity (smolts/spawner) and carrying capacity (smolts/km)	stochastic	Hierarchical Bayesian Model (HBM) Analysis
MS	Average marine survival rate applied over simulation to all populations	Good-0.06 Avg.-0.04 Poor-0.01	See text
δ	Maximum straying rate from a population when spawner density is high		See text
ϕ	Spawner density when straying rate is 50% of maximum δ)		See test
σ_f	SD of freshwater survival rate	stochastic	From HBM analysis
σ_m	SD of marine survival rate	0.57	SD from GBW/LF composite stock
$\rho_{y,f}$	Temporal autocorrelation (lag 1) in residuals from freshwater stock-recruitment curve	0.26	Mean lag-1 correlation of 16 populations used in HBM analysis
$\rho_{y,m}$	Temporal autocorrelation (lag 1) in residuals around average marine survival rate	0.57	Mean lag-1 correlation of 6 index stocks
$\rho_{p,f}$	Correlation of residuals of freshwater stock-recruitment curve among populations	0.29	Correlation among 16 populations used in HBM analysis
$\rho_{p,m}$	Correlation of residuals around mean marine survival rate among populations	0.71	Mean correlation among 6 index stocks

Symbol	PARAMETER	VALUE	Source
MANAGEMENT PARAMETERS			
σ_{κ}	SD of recruitment forecast	0.5	Simpson et al. 2004
σ_{λ}	SD of mean harvest rate	0.25	Uncertain, range of values examined
σ_{η}	SD of population specific harvest rate	0.25	Uncertain, range of values examined

Table 2. Summary of model scenarios. See Table 1 and text for definition of model parameters. For brevity, 'k' is used to denote units in thousands.

Scenario Type	Scenario Code	Description	Parameters			
Harvest	H1	Fixed harvest rate policy	NA	NA	$H_{min}=H_{max}$ (0.1-0.8)	
	H2	Abundance-based harvest rate with conservative (high) value of R_{min}	R_{min}=25 k	R_{max}=25, 48, or 73 k	H_{min}=0.1	H_{max}=0.6
	H3	Abundance-based harvest rate with aggressive (low) value of R_{min}	R_{min}=7.2 k	R_{max}=25, 48, or 73 k	H_{min}=0.1	H_{max}=0.6
	H4	PSC-type harvest rate	Harvest rates of 0.1, 0.3, and 0.6 at 24, 78 and 87 k recruits			
	H5	PSC-type quota	Quota of 10, 29, and 58 k at 24, 78, and 87 k recruits			
Marine Survival	M1	Poor	MS=0.01			
Rate	M2	Average	MS=0.04			
	M3	Good	MS=0.06			
Conservation	C1	Sensitive	Conservation limit = 19 sp/km, Extirpation limit = 6 sp/km			
Limits	C2	Default	Conservation limit = 6 sp/km, Extirpation limit = 2 sp/km			
Population	P1	Thompson-random (default)	8 populations, random stream length assignment			
Structure	P2	Thompson-fixed	8 populations, fixed stream lengths			
	P3	GBW less	24 populations, random stream length assignment			

Scenario Type	Scenario Code	Description	Parameters
	P4	GBW more	50 populations, random stream length assignment
Straying	S1	No straying	24 populations, δ=0
	S2	Density-dependent straying (low)	24 populations, δ=0.2, ϕ=50 sp/km
	S3	Density-dependent straying (high)	24 populations, δ=0.4, ϕ=50 sp/km
	S4	Density-independent straying	24 populations, δ=0.2, ϕ=0.01 sp/km
Variation in	V1	Default	Table 1: σ_m=0.57, $\rho_{y,f}$=0.26, $\rho_{y,m}$=0.57, $\rho_{p,f}$=0.29, $\rho_{p,m}$=0.71
Marine	V2	Increased variation in marine survival	σ_m=0.9
Survival Rate	V3	Increased autocorrelation in marine surv.	$\rho_{y,m}$=0.9
	V4	Increased correlation among populations in marine survival	$\rho_{p,m}$=0.9
Management	E1	Default	Table 1: σ_κ=0.5, σ_λ=0.25, σ_η=0.25
Error	E2	No forecast error	σ_κ=0, σ_λ=0.25, σ_η=0.25
	E3	Increased forecast error	σ_κ=1.0, σ_λ=0.25, σ_η=0.25
	E4	No implementation error	σ_κ=0.5, σ_λ=0, σ_η=0
	E5	Increased implementation error	σ_κ=0.5, σ_λ=0.5, σ_η=0.5

9. FIGURES

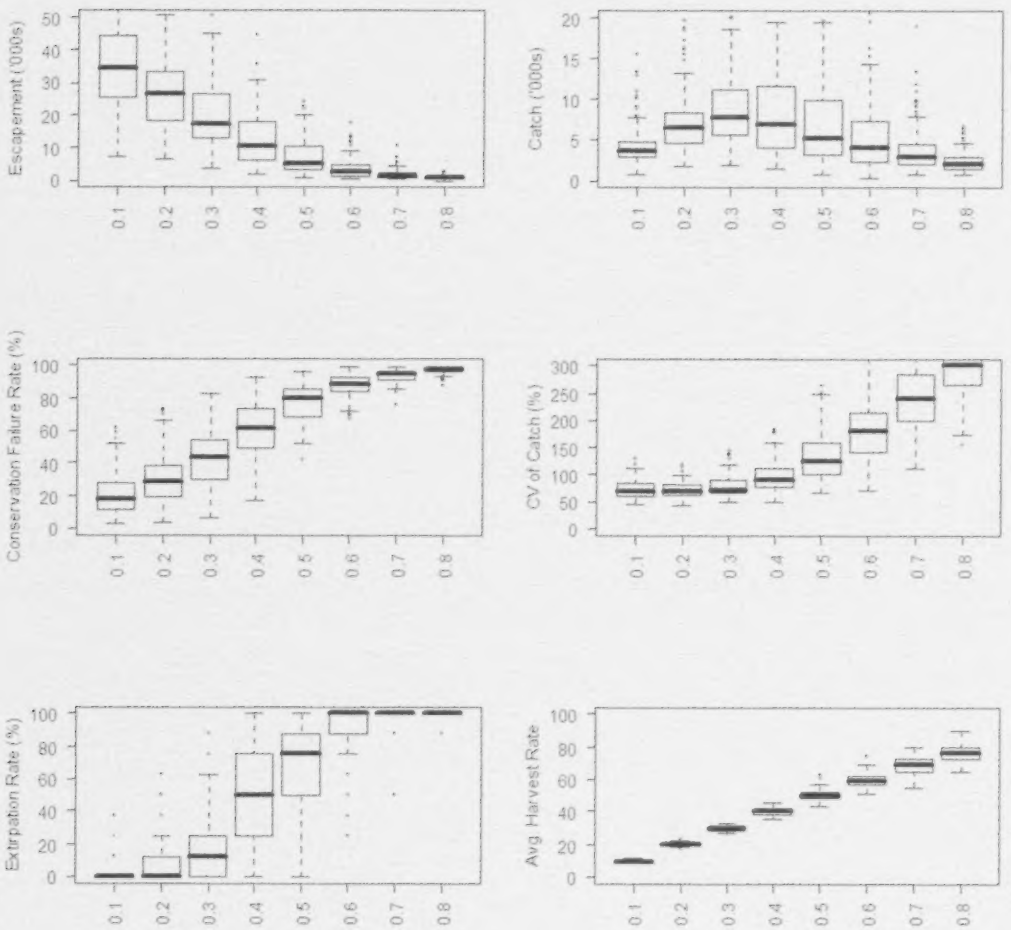

Figure 1. Box plots showing distributions of (from upper-left to lower-right) annual total escapement, annual catch, conservation failure rate, inter-annual coefficient of variation in catch (CV), extirpation rate, and realized average harvest rate under a range of fixed harvest rates (scenario H1 of Table 2). Distributions are based on 1000 simulation trials for each harvest rate under the default model scenario (M2, C2, P1, S2, V1, E1 from Table2). The thick horizontal line represents the median while the upper and lower ends of the box represent the first and third quartile, respectively. The whiskers extend to the most extreme data point that is within a distance of 1.5-fold of the interquartile range (the box width). Points represent outliers (> 1.5-fold of the interquartile range). See http://en.wikipedia.org/wiki/Box_plot for a more detailed description of box plots.

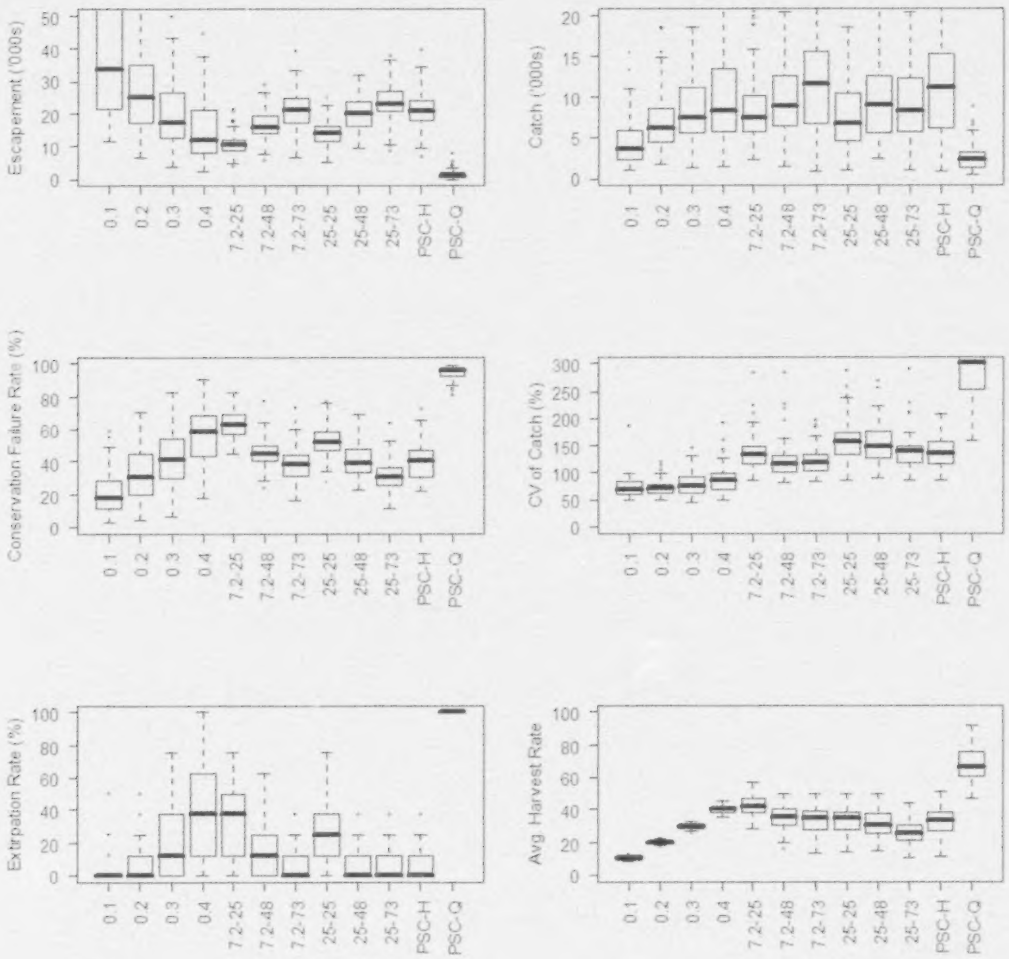

Figure 2. Box plots showing distributions of annual total escapement, annual catch, conservation failure rate, inter-annual coefficient of variation (CV) in catch, extinction rate, and realized average harvest rate under a range of fixed harvest rates (0.1-0.4) as well as abundance-based harvest policies (H2-H5, PSC-H, and PSC-Q of Table 2). Distributions are based on 1000 simulation trials under default model scenarios (M2, C2, P1, S2, V1, E1 from Table 2). Harvest policies with two numbers (e.g., 7.2-25) denote Rmin and Rmax values for the abundance-based harvest rate rules (H2 and H3, Table 2), while PSC-H and PSC-Q denote a Pacific Salmon Commission-type rule where harvest rate or quota varies across three 3 levels of abundance, respectively (Table 2).

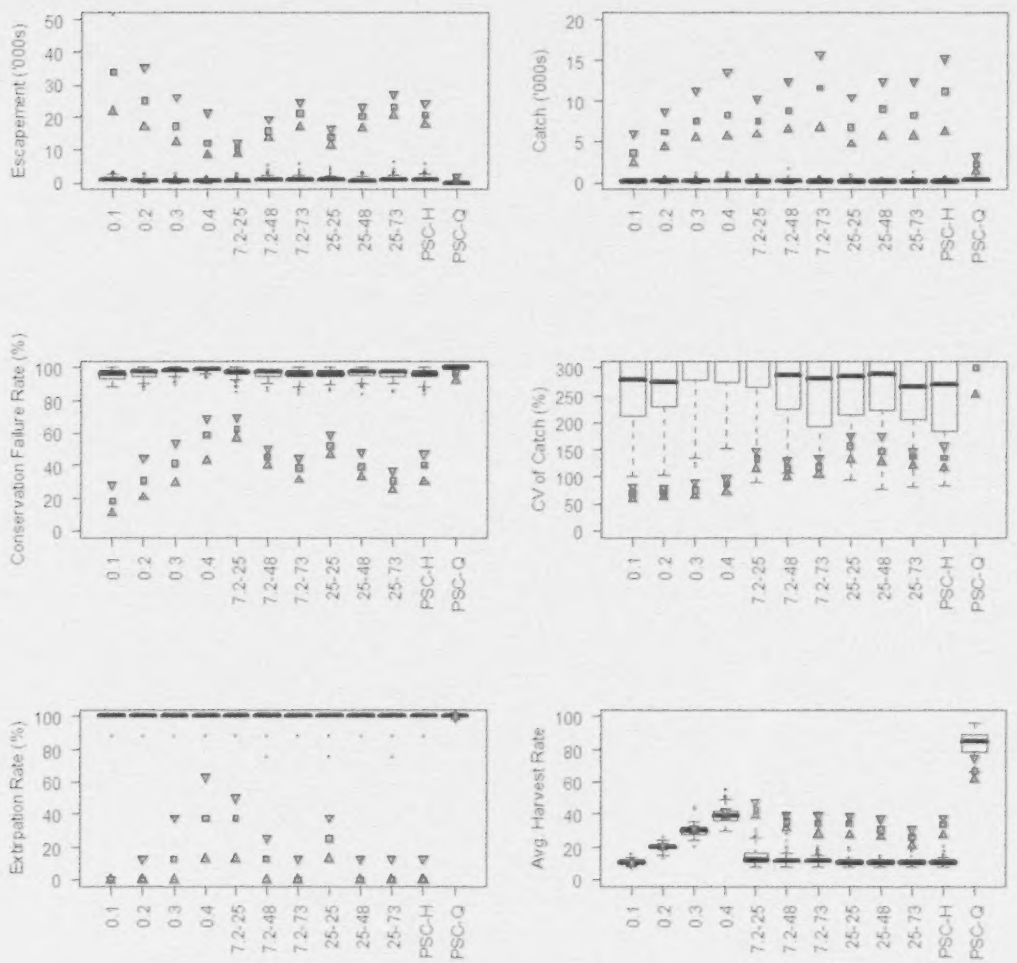

Figure 3. Box plots showing distributions of annual total escapement, annual catch, conservation failure rate, inter-annual coefficient of variation (CV) in catch, extinction rate, and realized average harvest rate under a range of fixed harvest rates (0.1-0.4) as well as abundance-based harvest policies (H2-H5, PSC-H, and PSC-Q of Table 2). Distributions are based on 1000 simulation trials under the low marine survival scenario (M1, C2, P1, S2, V1, E1 from Table 2). The red triangle, square, and inverted triangle represent the lower quartile, median and upper quartile from the default model scenarios (Fig. 2, scenarios M2, C2, P1, S2, V1, E1 from Table 2), respectively. See caption for Fig. 1 for additional details.

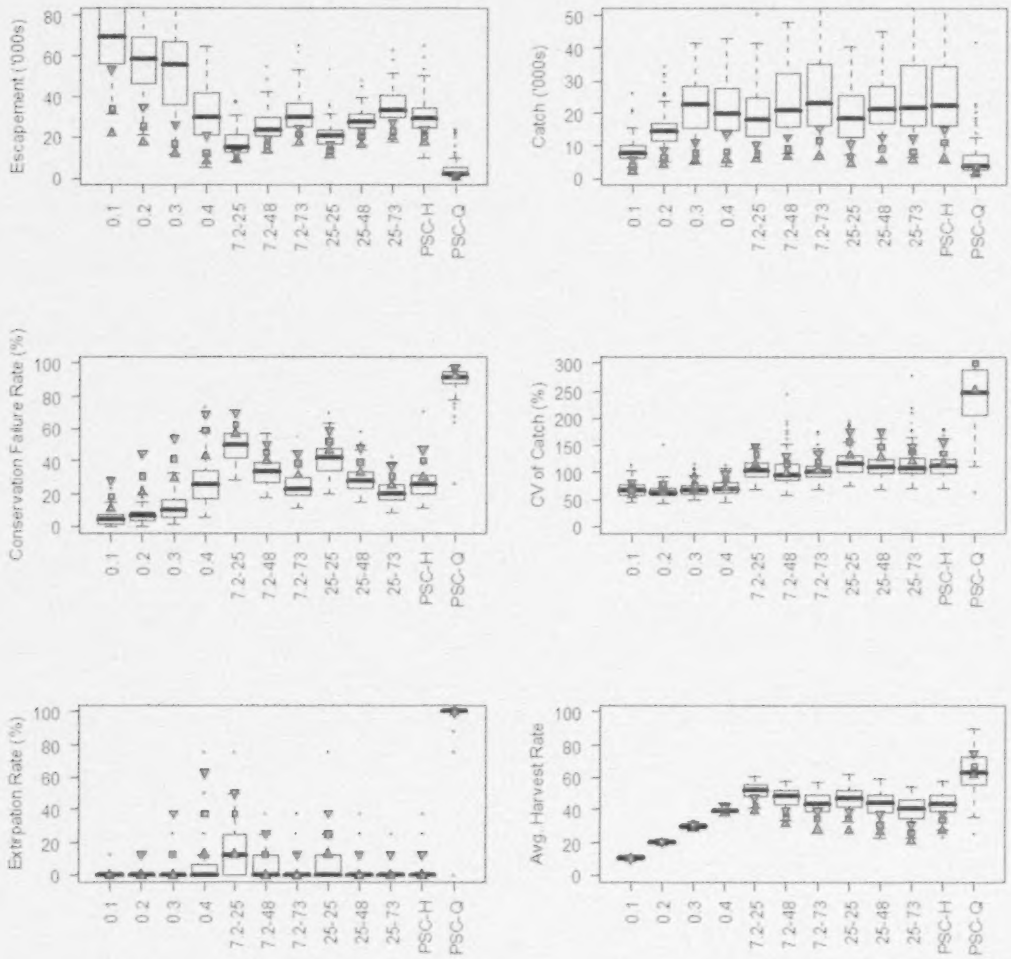

Figure 4. Box plots showing distributions of annual total escapement, annual catch, conservation failure rate, inter-annual coefficient of variation (CV) in catch, extinction rate, and realized average harvest rate under a range of fixed harvest rates (0.1-0.4) as well as abundance-based harvest policies (H2-H5, PSC-H, and PSC-Q of Table 2). Distributions are based on 1000 simulation trials under the high marine survival scenario (M3, C2, P1, S2, V1, E1 from Table 2). The red triangle, square, and inverted triangle represent the lower quartile, median and upper quartile from the default model scenarios (Fig. 2, scenarios M2, C2, P1, S2, V1, E1 from Table 2), respectively. See caption for Fig. 1 for additional details.

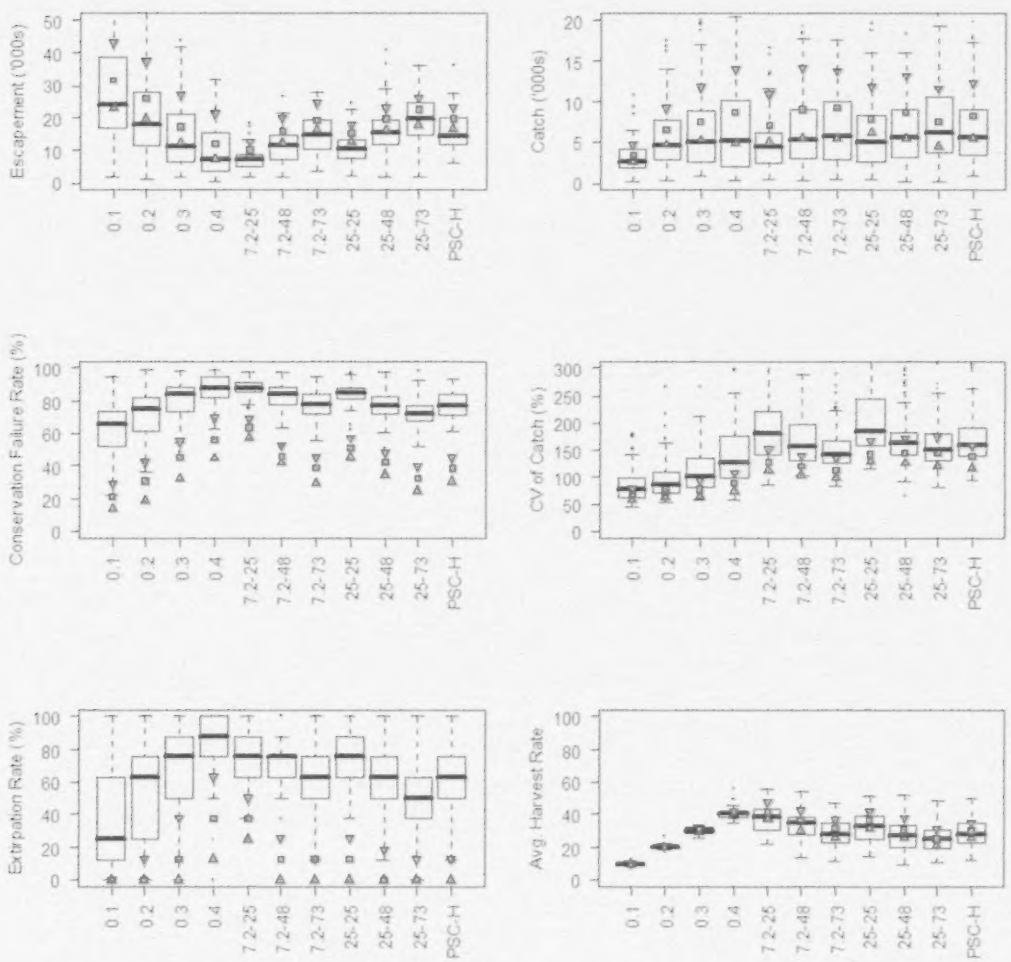

Figure 5. Box plots showing distributions of annual total escapement, annual catch, conservation failure rate, inter-annual coefficient of variation (CV) in catch, extinction rate, and realized average harvest rate under a range of fixed harvest rates (0.1-0.4) as well as abundance-based harvest policies (H2-H5, and PSC-H of Table 2). Distributions are based on 1000 simulation trials under the sensitive conservation scenario (M2, C1, P1, S2, V1, E1 from Table 2). The red triangle, square, and inverted triangle represent the lower quartile, median and upper quartile from the default model scenario (Fig. 2, scenarios M2, C2, P1, S2, V1, E1 from Table 2), respectively. See caption for Fig. 1 for additional details.

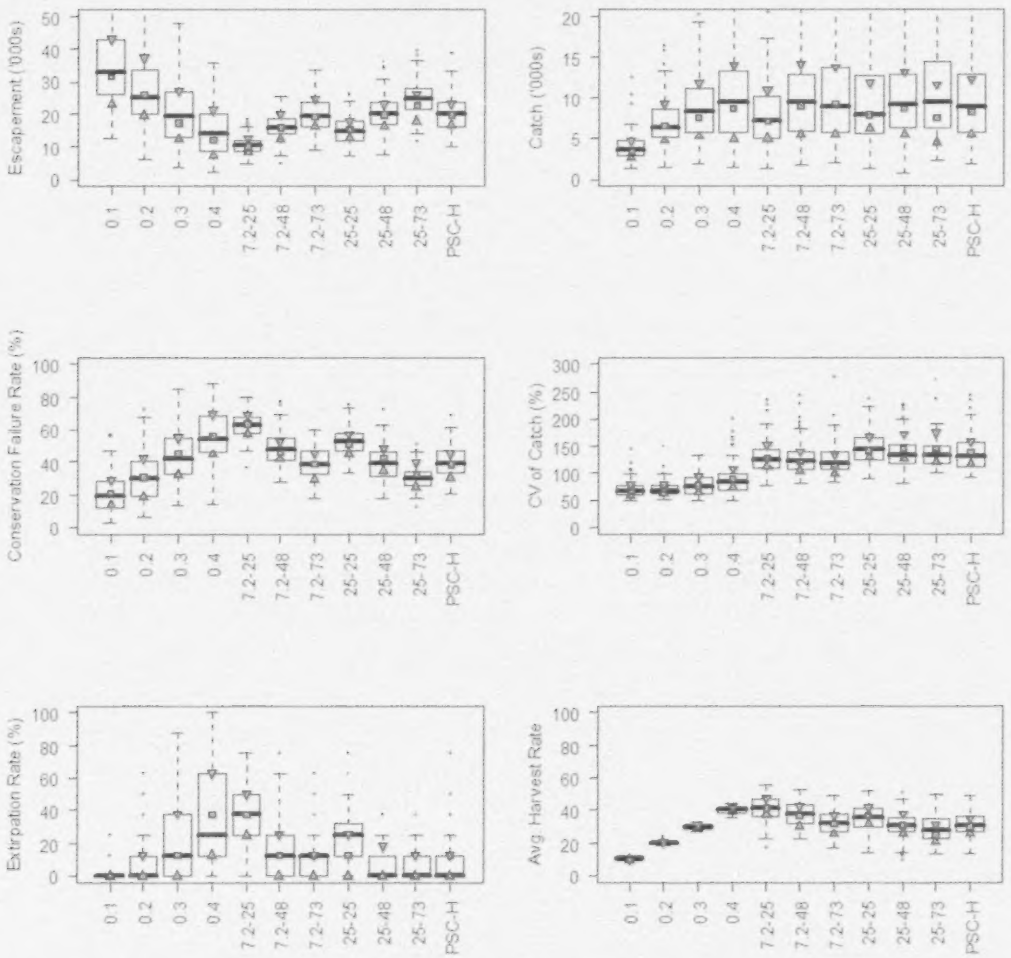

Figure 6. Box plots showing distributions of annual total escapement, annual catch, conservation failure rate, inter-annual coefficient of variation (CV) in catch, extinction rate, and realized average harvest rate under a range of fixed harvest rates (0.1-0.4) as well as abundance-based harvest policies (H2-H5, and PSC-H of Table 2). Distributions are based on 1000 simulation trials under the scenario where stream lengths were not randomly assigned to populations (M2, C2, P2, S2, V1, E1 from Table 2). The red triangle, square, and inverted triangle represent the lower quartile, median and upper quartile from the default model scenario (Fig. 2, scenarios M2, C2, P1, S2, V1, E1 from Table 2), respectively. See caption for Fig. 1 for additional details.

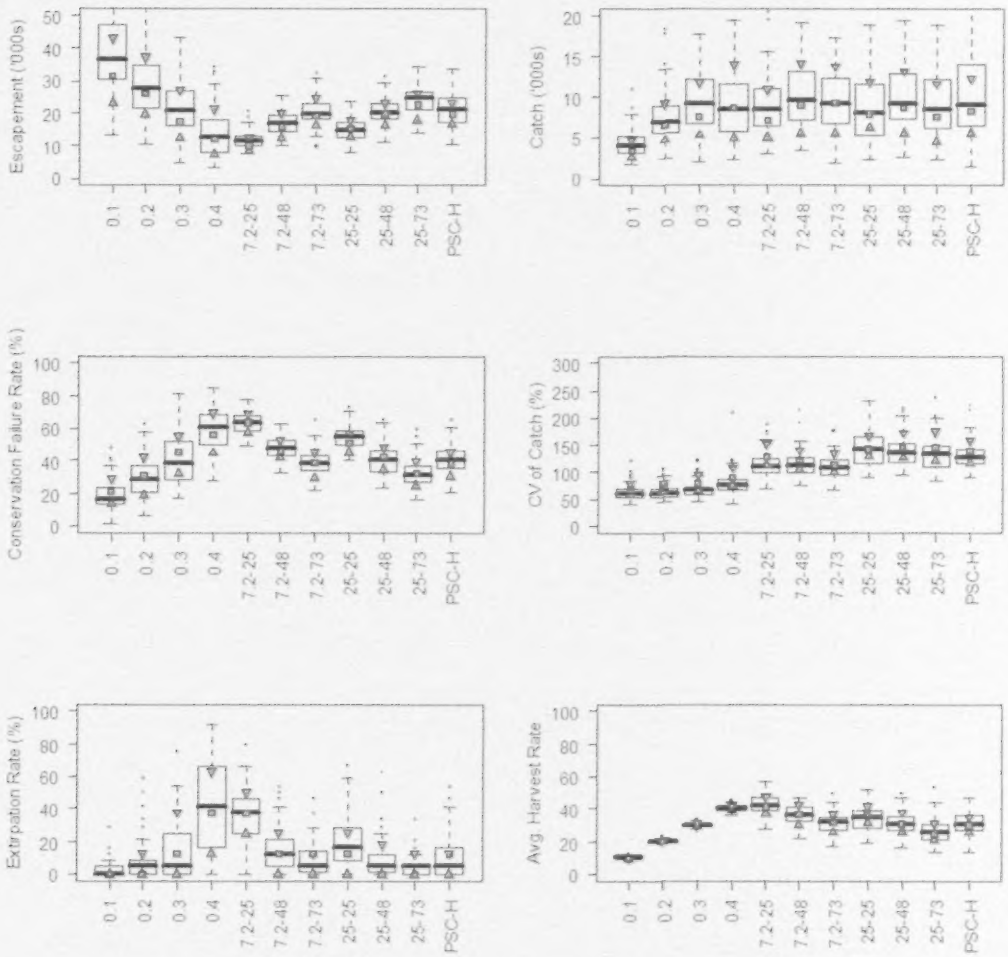

Figure 7. Box plots showing distributions of annual total escapement, annual catch, conservation failure rate, inter-annual coefficient of variation (CV) in catch, extinction rate, and realized average harvest rate under a range of fixed harvest rates (0.1-0.4) as well as abundance-based harvest policies (H2-H5, and PSC-H of Table 2). Distributions are based on 1000 simulation trials under the scenario where 25 populations were simulated (M2, C2, P3, S2, V1, E1 from Table 2). The red triangle, square, and inverted triangle represent the lower quartile, median and upper quartile from the default model scenario (Fig. 2, scenarios M2, C2, P1, S2, V1, E1 from Table 2), respectively. See caption for Fig. 1 for additional details.

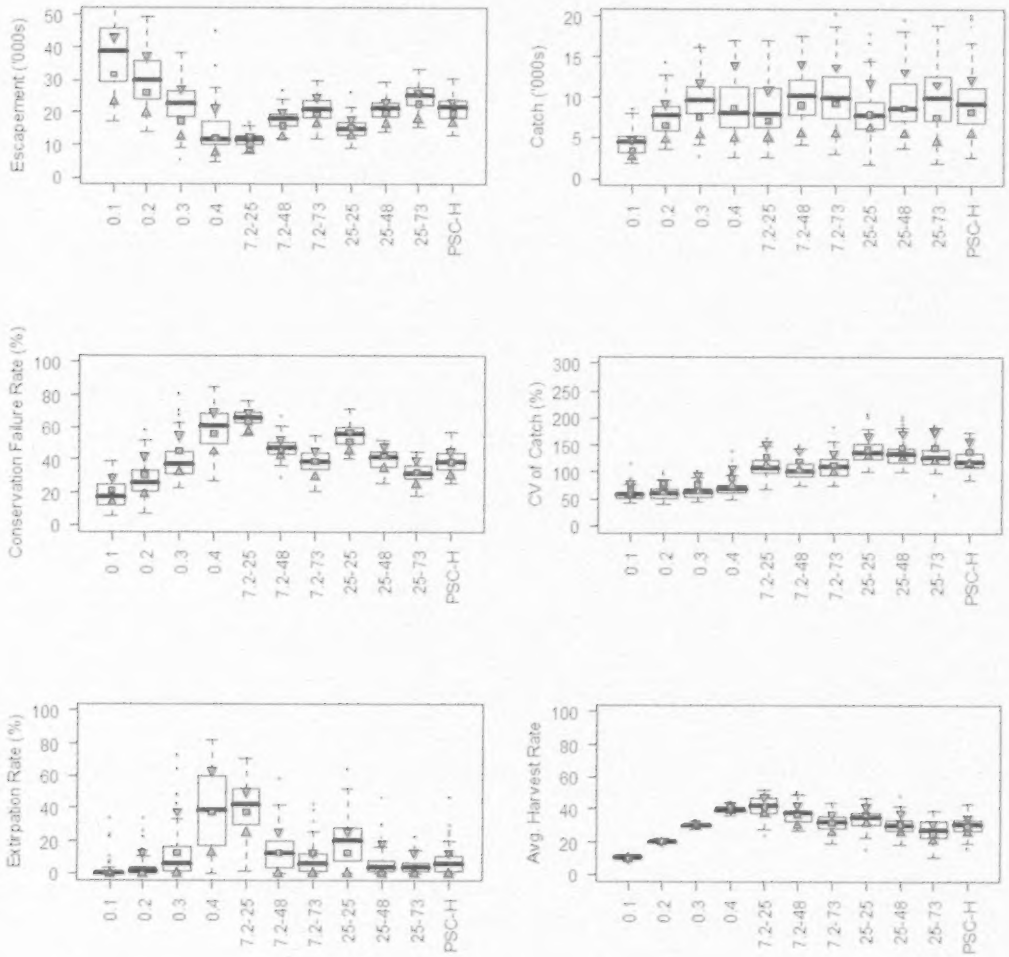

Figure 8. Box plots showing distributions of annual total escapement, annual catch, conservation failure rate, inter-annual coefficient of variation (CV) in catch, extinction rate, and realized average harvest rate under a range of fixed harvest rates (0.1-0.4) as well as abundance-based harvest policies (H2-H5, and PSC-H of Table 2). Distributions are based on 1000 simulation trials under the scenario where 50 populations were simulated (M2, C2, P4, S2, V1, E1 from Table 2). The red triangle, square, and inverted triangle represent the lower quartile, median and upper quartile from the default model scenario (Fig. 2, scenarios M2, C2, P1, S2, V1, E1 from Table 2), respectively. See caption for Fig. 1 for additional details.

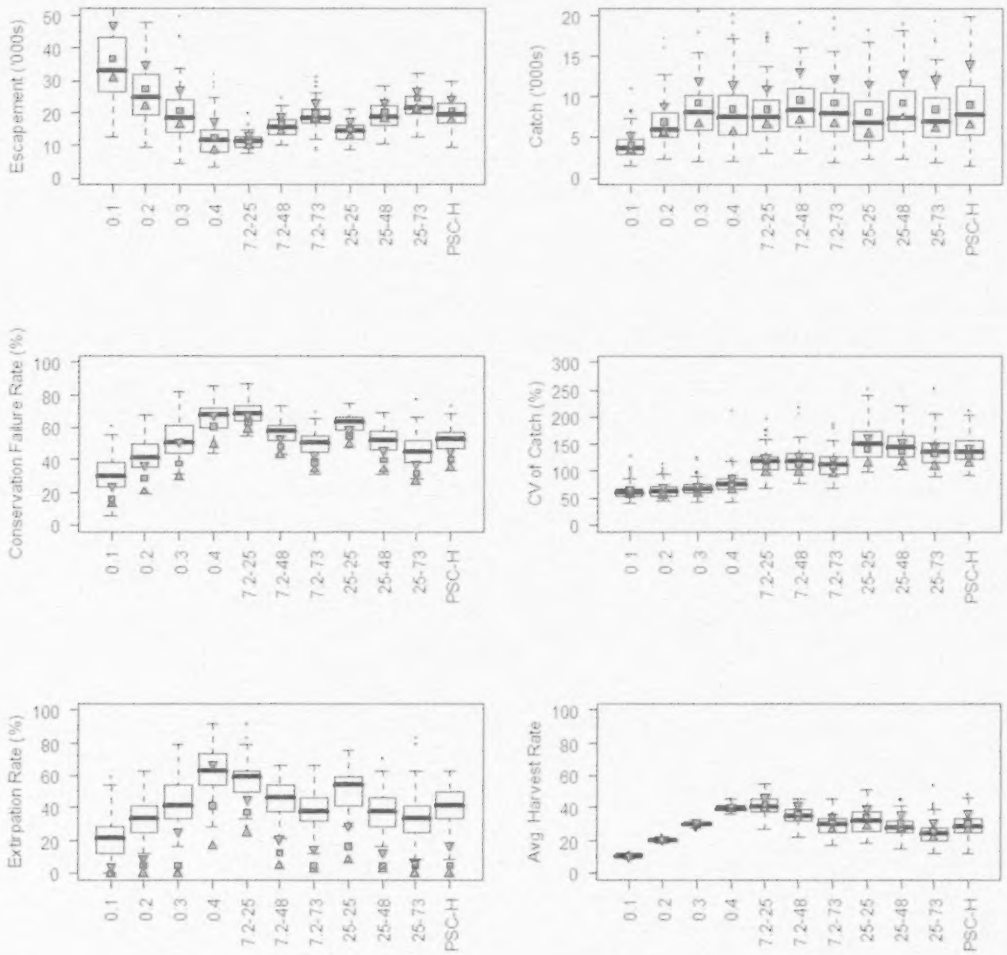

Figure 9. Box plots showing distributions of annual total escapement, annual catch, conservation failure rate, inter-annual coefficient of variation (CV) in catch, extinction rate, and realized average harvest rate under a range of fixed harvest rates (0.1-0.4) as well as abundance-based harvest policies (H2-H5, and PSC-H of Table 2). Distributions are based on 1000 simulation trials under the scenario without straying and where 24 populations were simulated (M2, C2, P3, S1, V1, E1 from Table 2). The red triangle, square, and inverted triangle represent the lower quartile, median and upper quartile from the model scenario where 25 populations were simulated (Fig. 2, scenarios M2, C2, P3, S2, V1, E1 from Table 2), respectively. See caption for Fig. 1 for additional details.

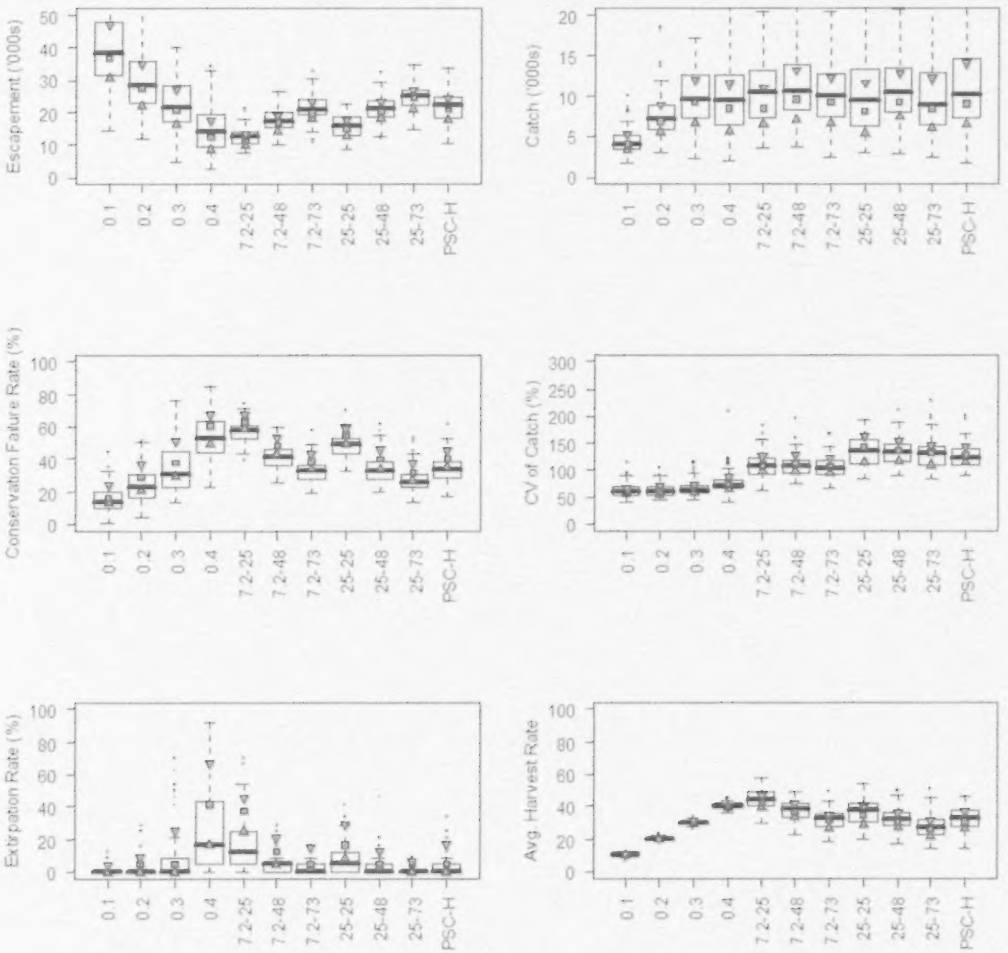

Figure 10. Box plots showing distributions of annual total escapement, annual catch, conservation failure rate, inter-annual coefficient of variation (CV) in catch, extinction rate, and realized average harvest rate under a range of fixed harvest rates (0.1-0.4) as well as abundance-based harvest policies (H2-H5, and PSC-H of Table 2). Distributions are based on 1000 simulation trials under the scenario with high straying and where 24 populations were simulated (M2, C2, P3, S3, V1, E1 from Table 2). The red triangle, square, and inverted triangle represent the lower quartile, median and upper quartile from the model scenario where 24 populations were simulated (Fig. 2, scenarios M2, C2, P3, S2, V1, E1 from Table 2), respectively. See caption for Fig. 1 for additional details.

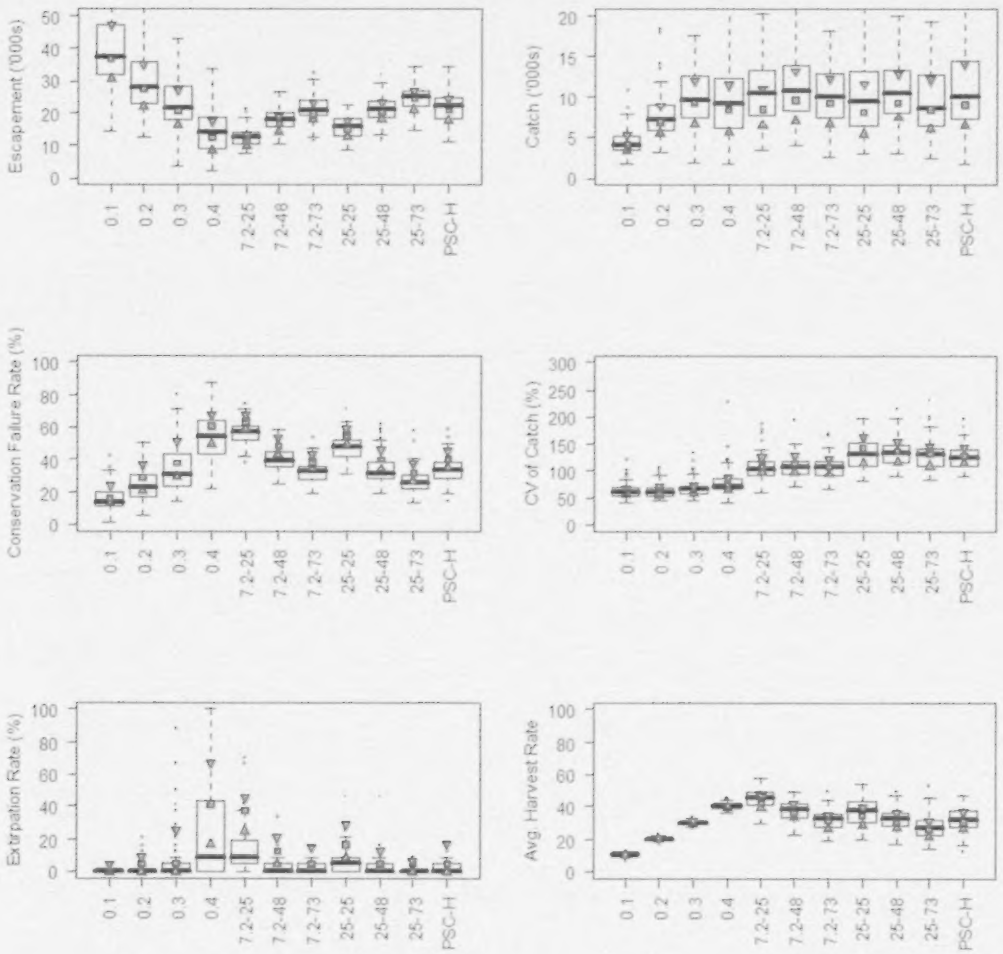

Figure 11. Box plots showing distributions of annual total escapement, annual catch, conservation failure rate, inter-annual coefficient of variation (CV) in catch, extinction rate, and realized average harvest rate under a range of fixed harvest rates (0.1-0.4) as well as abundance-based harvest policies (H2-H5, and PSC-H of Table 2). Distributions are based on 1000 simulation trials under the scenario with density-independent straying and where 24 populations were simulated (M2, C2, P3, S4, V1, E1 from Table 2). The red triangle, square, and inverted triangle represent the lower quartile, median and upper quartile from the model scenario where 24 populations were simulated (Fig. 2, scenarios M2, C2, P3, S2, V1, E1 from Table 2), respectively. See caption for Fig. 1 for additional details.

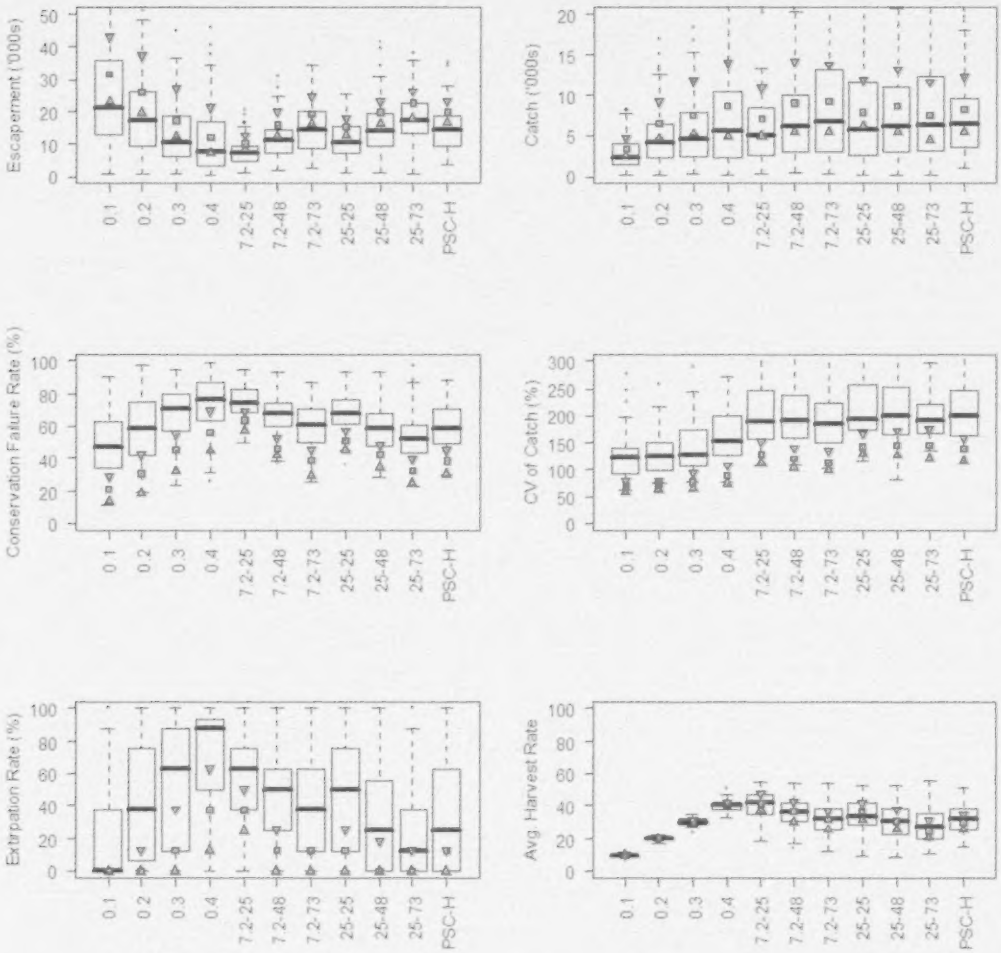

Figure 12. Box plots showing distributions of annual total escapement, annual catch, conservation failure rate, inter-annual coefficient of variation (CV) in catch, extinction rate, and realized average harvest rate under a range of fixed harvest rates (0.1-0.4) as well as abundance-based harvest policies (H2-H5, and PSC-H of Table 2). Distributions are based on 1000 simulation trials under the scenario with high inter-annual variation in marine survival rates (M2, C2, P1, S2, V2, E1 from Table 2). The red triangle, square, and inverted triangle represent the lower quartile, median and upper quartile from the default model scenarios (Fig. 2, scenarios M2, C2, P1, S2, V1, E1 from Table 2), respectively. See caption for Fig. 1 for additional details.

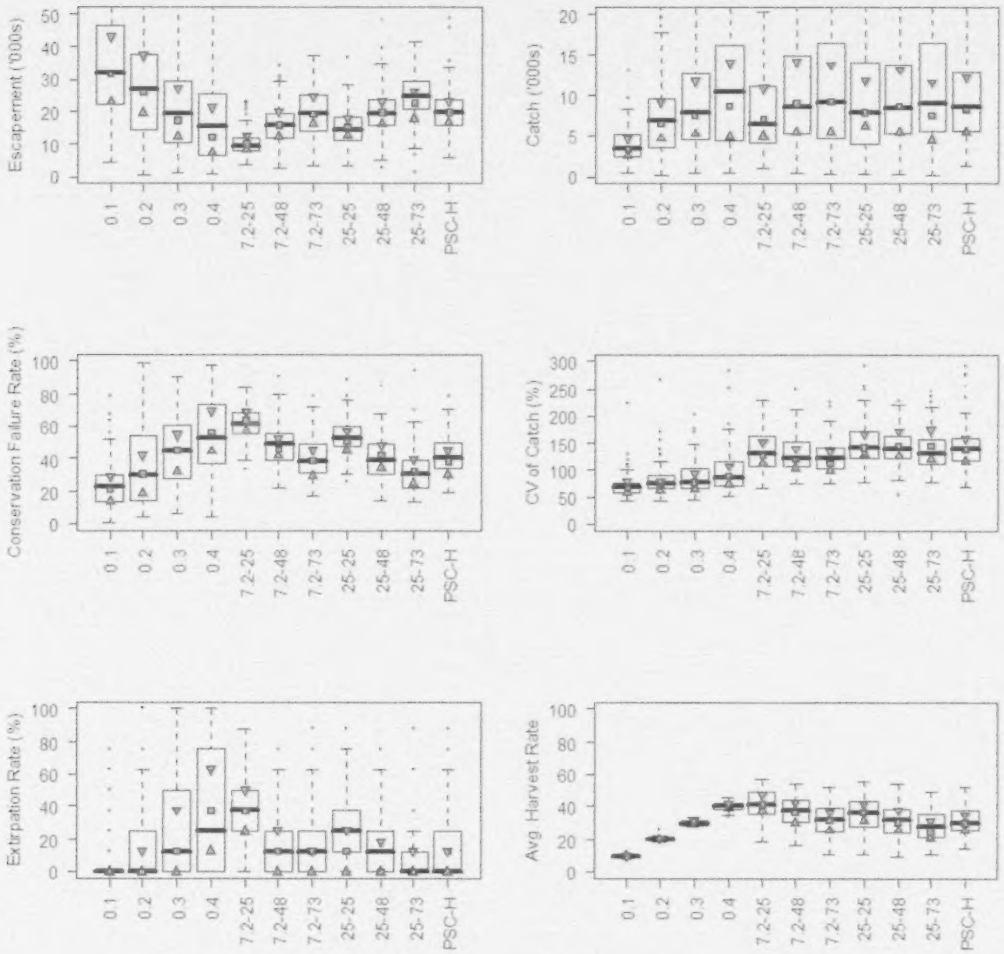

Figure 13. Box plots showing distributions of annual total escapement, annual catch, conservation failure rate, inter-annual coefficient of variation (CV) in catch, extinction rate, and realized average harvest rate under a range of fixed harvest rates (0.1-0.4) as well as abundance-based harvest policies (H2-H5, and PSC-H of Table 2). Distributions are based on 1000 simulation trials under the scenario with high temporal autocorrelation in marine survival rates (M2, C2, P1, S2, V3, E1 from Table 2). The red triangle, square, and inverted triangle represent the lower quartile, median and upper quartile from the default model scenarios (Fig. 2, scenarios M2, C2, P1, S2, V1, E1 from Table 2), respectively. See caption for Fig. 1 for additional details.

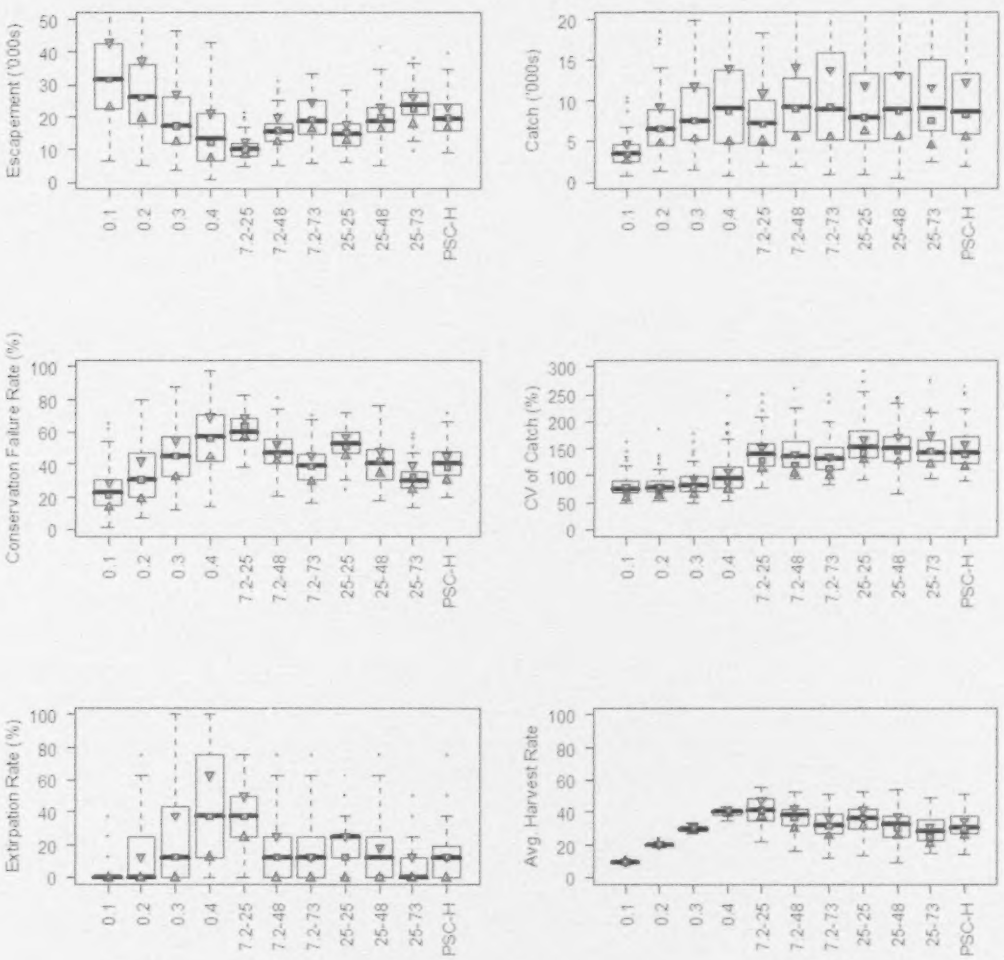

Figure 14. Box plots showing distributions of annual total escapement, annual catch, conservation failure rate, inter-annual coefficient of variation (CV) in catch, extinction rate, and realized average harvest rate under a range of fixed harvest rates (0.1-0.4) as well as abundance-based harvest policies (H2-H5, and PSC-H of Table 2). Distributions are based on 1000 simulation trials under the scenario with high inter-stock correlation in marine survival rates (M2, C2, P1, S2, V4, E1 from Table 2). The red triangle, square, and inverted triangle represent the lower quartile, median and upper quartile from the default model scenarios (Fig. 2, scenarios M2, C2, P1, S2, V1, E1 from Table 2), respectively. See caption for Fig. 1 for additional details.

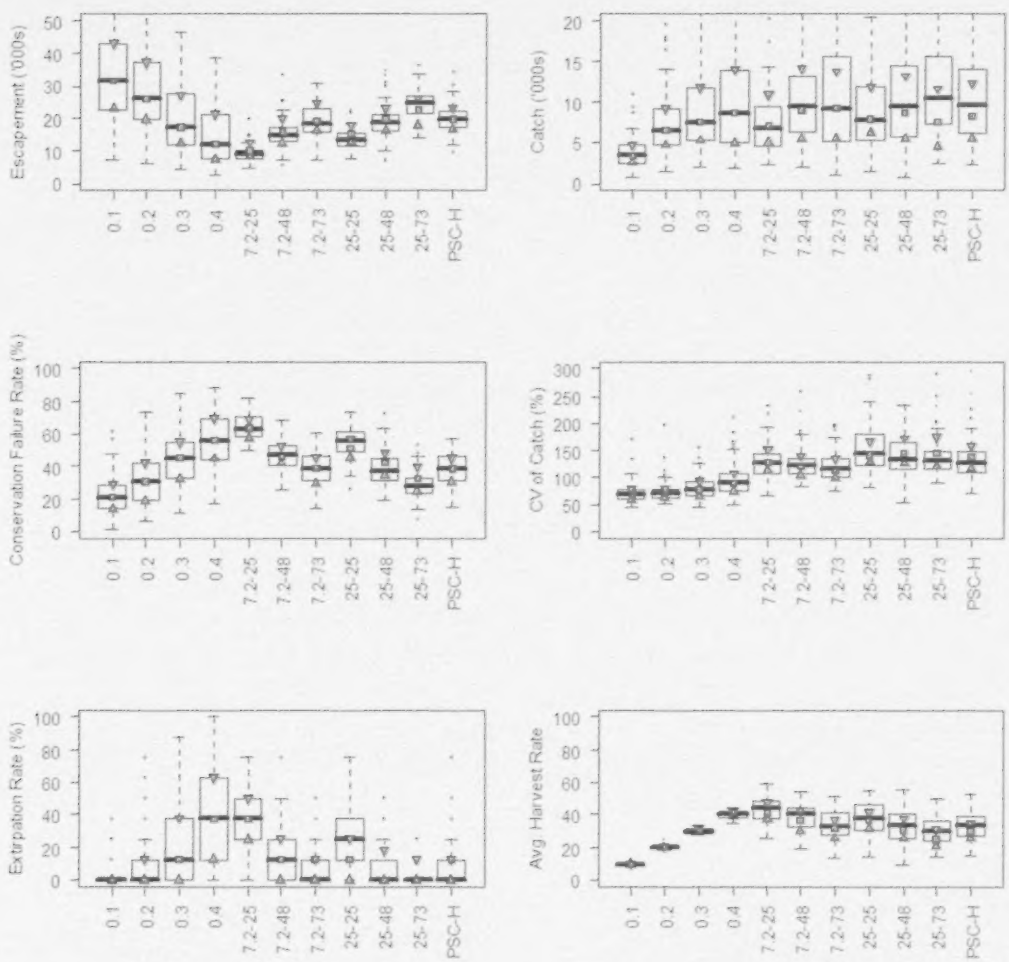

Figure 15. Box plots showing distributions of annual total escapement, annual catch, conservation failure rate, inter-annual coefficient of variation (CV) in catch, extinction rate, and realized average harvest rate under a range of fixed harvest rates (0.1-0.4) as well as abundance-based harvest policies (H2-H5, and PSC-H of Table 2). Distributions are based on 1000 simulation trials under the scenario with no error in recruitment forecasts used to determine harvest rates for abundance-based rules (M2, C2, P1, S2, V1, E2 from Table 2). The red triangle, square, and inverted triangle represent the lower quartile, median and upper quartile from the default model scenarios (Fig. 2, scenarios M2, C2, P1, S2, V1, E1 from Table 2), respectively. See caption for Fig. 1 for additional details.

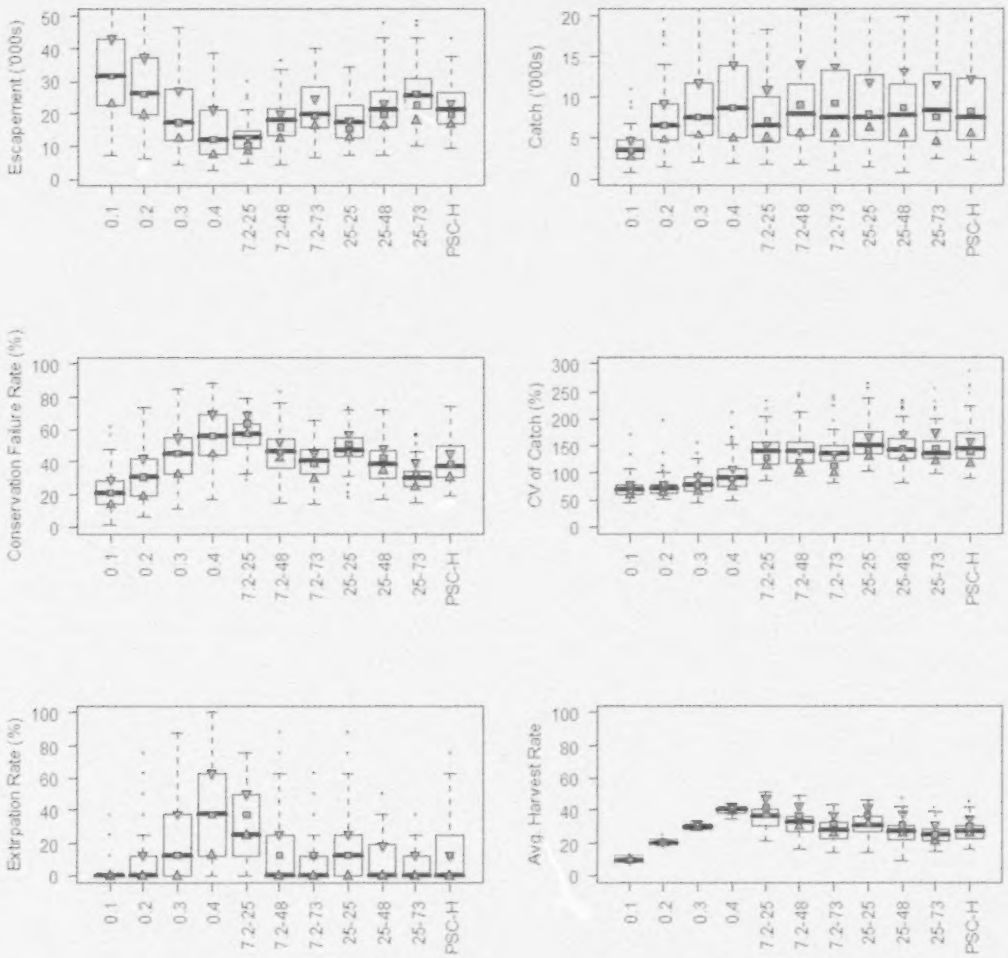

Figure 16. Box plots showing distributions of annual total escapement, annual catch, conservation failure rate, inter-annual coefficient of variation (CV) in catch, exploitation rate, and realized average harvest rate under a range of fixed harvest rates (0.1-0.4) as well as abundance-based harvest policies (H2-H5, and PSC-H of Table 2). Distributions are based on 1000 simulation trials under the scenario with high error in recruitment forecasts used to determine harvest rates for abundance-based rules (M2, C2, P1, S2, V1, E3 from Table 2). The red triangle, square, and inverted triangle represent the lower quartile, median and upper quartile from the default model scenarios (Fig. 2, scenarios M2, C2, P1, S2, V1, E1 from Table 2), respectively. See caption for Fig. 1 for additional details.

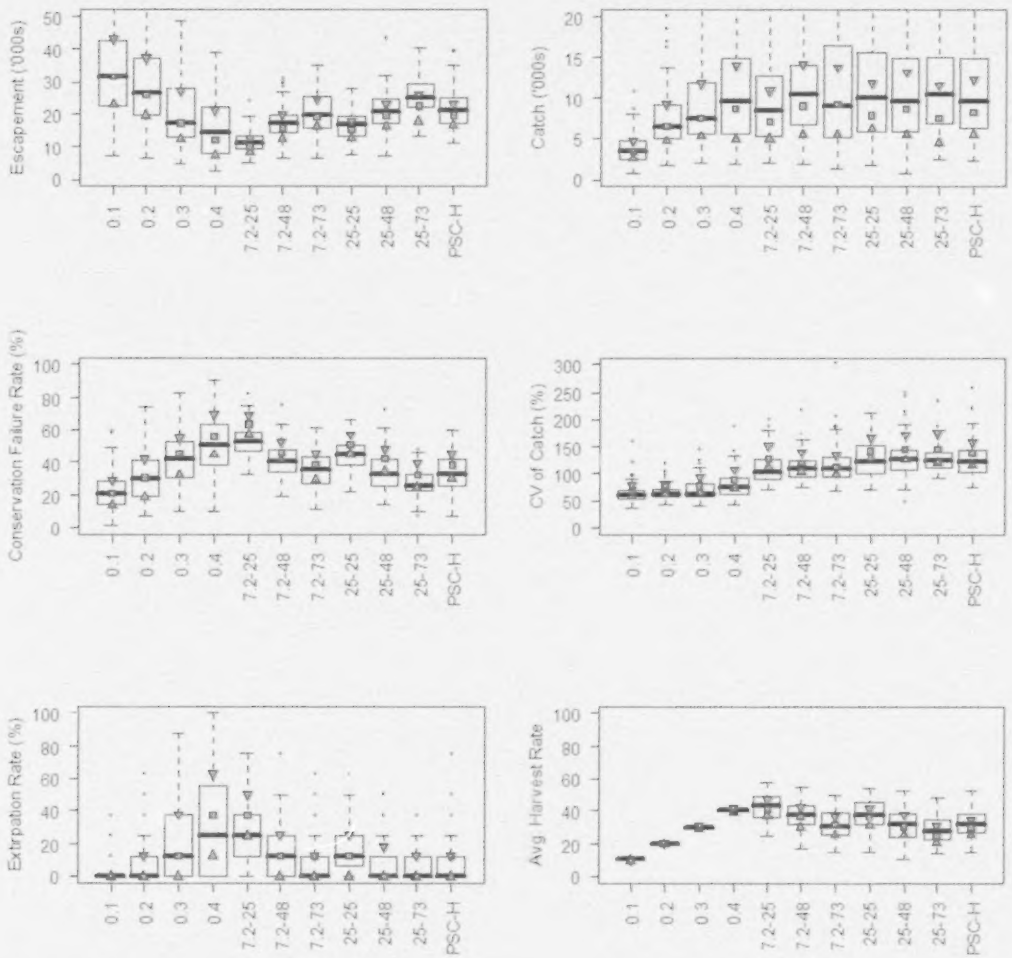

Figure 17. Box plots showing distributions of annual total escapement, annual catch, conservation failure rate, inter-annual coefficient of variation (CV) in catch, extinction rate, and realized average harvest rate under a range of fixed harvest rates (0.1-0.4) as well as abundance-based harvest policies (H2-H5, and PSC-H of Table 2). Distributions are based on 1000 simulation trials under the scenario with no implementation error in target harvest rates (M2, C2, P1, S2, V1, E4 from Table 2). The red triangle, square, and inverted triangle represent the lower quartile, median and upper quartile from the default model scenarios (Fig. 2, scenarios M2, C2, P1, S2, V1, E1 from Table 2), respectively. See caption for Fig. 1 for additional details.

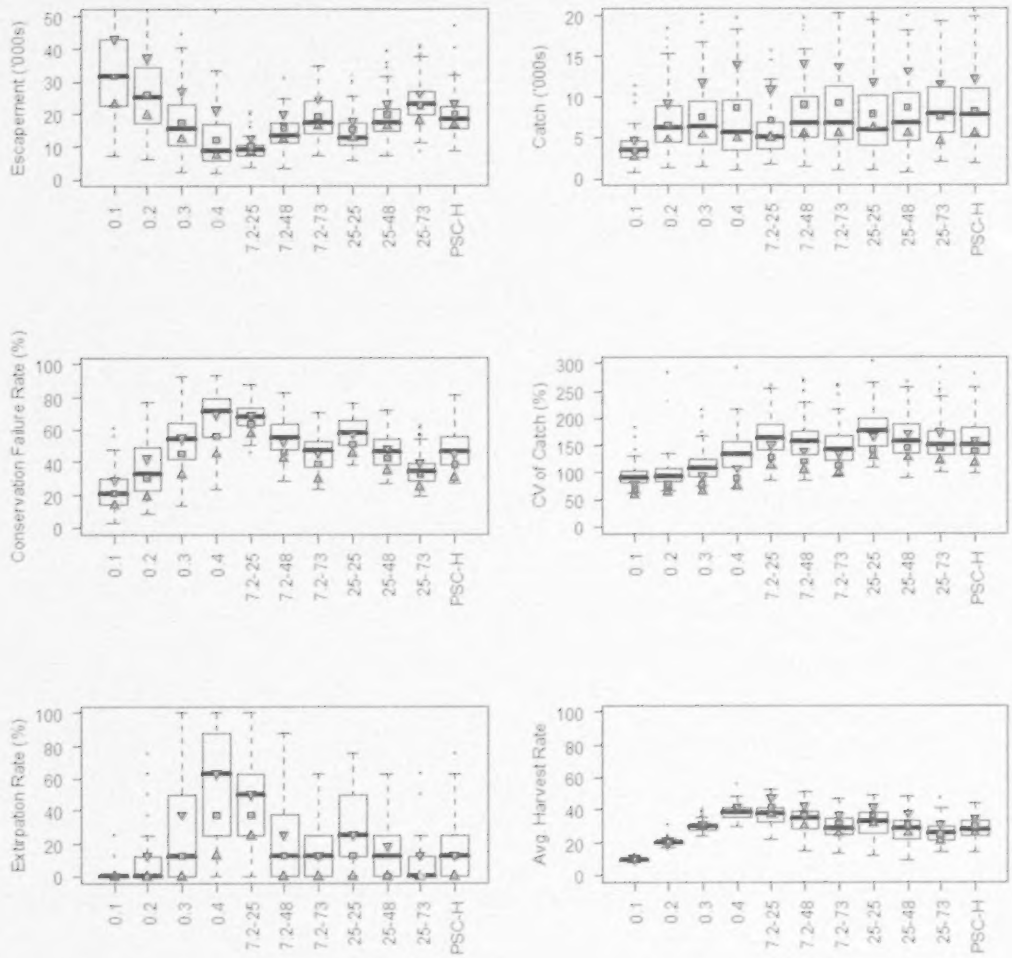

Figure 18. Box plots showing distributions of annual total escapement, annual catch, conservation failure rate, inter-annual coefficient of variation (CV) in catch, extinction rate, and realized average harvest rate under a range of fixed harvest rates (0.1-0.4) as well as abundance-based harvest policies (H2-H5, and PSC-H of Table 2). Distributions are based on 1000 simulation trials under the scenario with high error in implementation of target harvest rates (M2, C2, P1, S2, V1, E5 from Table 2). The red triangle, square, and inverted triangle represent the lower quartile, median and upper quartile from the default model scenarios (Fig. 2, scenarios M2, C2, P1, S2, V1, E1 from Table 2), respectively. See caption for Fig. 1 for additional details.